

Appendix E
**Effects of LEAPS Operation
on Lake Elsinore – Predictions
from 3-D Hydrodynamic
Modeling**

This page intentionally left blank.

**EFFECTS OF LEAPS OPERATION ON LAKE ELSINORE:
PREDICTIONS FROM 3-D HYDRODYNAMIC MODELING**

DRAFT FINAL REPORT

Submitted to:

Santa Ana Regional Water Quality Control Board
3737 Main St.
Suite 500
Riverside, CA 92501

Submitted by:

Michael A. Anderson
Department of Environmental Sciences
University of California, Riverside

23 April 2007

Table of Contents

Executive Summary	1
1.0 Introduction	4
2.0 EFDC Model	4
2.1 Model Calibration	5
2.2 Model Verification.....	10
3.0 LEAPS Simulations	13
3.1 Flows.....	13
3.2 Intake Structure Design.....	14
4.0 Simulation Results	17
4.1 Lake Surface Elevation Changes During Operation	17
4.2 Velocities Near Intake	17
4.2.1 Predicted Velocities Near Intake at 1247 ft	18
4.2.2 Predicted Velocities Near Intake at 1240 ft	20
4.3 Bottom Shear and Sediment Resuspension	22
4.3.1 Predicted Bottom Shear at 1247 ft.....	22
4.3.2 Predicted Bottom Shear at 1240 ft.....	24
4.4 Effect on Stratification and Mixing.....	25
4.4.1 Stratification and Mixing at 1247 ft.....	25
4.4.2 Stratification and Mixing at 1240 ft.....	25
4.5 Selective Withdrawal.....	31
4.5.1 Velocities Near Intake	31
4.5.2 Bottom Shear and Sediment Resuspension	39
4.5.3 Stratification and Mixing	42
5.0 Discussion	43
6.0 Conclusions	47

7.0 References.....48

List of Figures

Fig. 1. Lake computational grid	5
Fig. 2. Meteorological conditions used in model calibration.....	6
Fig. 3. Predicted and observed surface and bottom water temperatures at site E2.	7
Fig. 4. Predicted and observed temperature profiles at site E2.	8
Fig. 5. Predicted and observed bottom water temperatures at ADV site.	9
Fig. 6. Predicted and observed bottom water velocities at the ADV site.....	10
Fig. 7. Water column temperatures at site E2: a) observed and b) predicted profiles ...	11
Fig. 8. Predicted and observed surface and bottom water temperatures at site E2.	12
Fig. 9. Supplemental flows to Lake Elsinore to maintain lake elevation.....	14
Fig. 10. Withdrawal and return flows due to LEAPS operation..	10
Fig. 11. Approximate longitudinal cross-section near intake: Santa Rosa site.	15
Fig. 12. Approximate longitudinal cross-section near intake: Ortega Oaks site.....	16
Fig. 13. Predicted elevation changes for Lake Elsinore during LEAPS operation.	17
Fig. 14. Predicted velocity field perpendicular to intake at the Santa Rosa site, 1247' ...	18
Fig. 15. Predicted velocity field perpendicular to intake at the Ortega Oaks site, 1247' .	20
Fig. 16. Predicted velocity field perpendicular to intake at the Santa Rosa site, 1240' ...	21
Fig. 17. Predicted velocity field perpendicular to intake at the Ortega Oaks site, 1240' .	22
Fig. 18. Predicted bottom shear at the Santa Rosa site at 1247'.....	23
Fig. 19. Predicted bottom shear at the Ortega Oaks site at 1247'	24
Fig. 20. Predicted bottom shear during generation at 1240'	25
Fig. 21. Predicted water column temperatures at site E2 without LEAPS (1247').	26
Fig. 22. Temperature differential, surface and bottom waters without LEAPS (1247'). ..	27
Fig. 23. Effect of LEAPS operation on predicted ΔT values, 1247'.....	28
Fig. 24. Temperature differential, surface and bottom waters without LEAPS (1240'). ..	29
Fig. 25. Effect fo LEAPS operation on predicted ΔT values, 1240'.....	30

Fig. 26. Predicted velocity field perpendicular to intake at the Santa Rosa site at 1247',
150 m x 1m intake gate. 32

Fig. 27. Predicted velocity field perpendicular to intake at the Santa Rosa site at 1247',
40 m x 1 m intake gate. 34

Fig. 28. Predicted velocity field perpendicular to intake at the Santa Rosa site at 1247',
10 m x 1 m intake gate. 35

Fig. 29. Predicted velocity field perpendicular to intake at the Ortega Oaks site at 1247',
150 m x 1m intake gate. 36

Fig. 30. Predicted velocity field perpendicular to intake at the Ortega Oaks site at 1247',
40 m x 1 m intake gate. 38

Fig. 31. Predicted velocity field perpendicular to intake at the Ortega Oaks site at 1247',
10 m x 1 m intake gate. 39

Fig. 32. Predicted bottom shear during generation at the Santa Rosa site, 1247', for 3
different gate dimensions. 40

Fig. 33. Predicted bottom shear during generation at the Ortega Oaks site, 1247', for 3
different gate dimensions. 41

Fig. 34. Effect of LEAPS operation on predicted ΔT values, 150 m x 1 m, 1247'. 42

Fig. 35. Effect fo LEAPS operation on predicted ΔT values, 40 m & 10 m x 1 m, 1247'. 43

List of Tables

Table 1. Error analysis for model validation. 12

Table 2. Intensity and duration of stratification at a lake elevation of 1247' with and without LEAPS operation. 29

Table 3. Intensity and duration of stratification at a lake elevation of 1240' with and without LEAPS operation. 30

Table 4. Predicted sediment resuspension at the Santa Rosa site (1247'). 40

Table 5. Predicted sediment resuspension at the Ortega Oaks site (1247')..... 41

Executive Summary

Three-dimensional hydrodynamic simulations were conducted using the Environmental Fluid Dynamics Code (EFDC) to evaluate the effects of operation of the proposed Lake Elsinore Advanced Pumped Storage project (LEAPS) on stratification, mixing and sediment resuspension in Lake Elsinore. A Cartesian 100 m x 100 m computational grid was constructed from available bathymetric data that yielded 1402 horizontal water cells. The vertical dimension was represented with an 8-layer sigma vertical coordinate system. The model was calibrated using available meteorological and water column data from the March – September 2006 period. This period was chosen because the lake level was approximately 1247', the proposed upper operating elevation of LEAPS. The model reasonably reproduced observed temperature profiles in the lake when the evaporative and convective heat flux constants were increased from default values of 1.5 to 2.0. The model also adequately reproduced temperature and velocity measurements made in the southwest corner of the lake. The model was then validated using data collected in 2001; this period was chosen for model validation-verification since the lake was much lower than the level during calibration (1241.5'), water column temperature profile measurements were available on 30-min intervals, and this lake level approached the nominal minimum operating level of 1240'. The model adequately reproduced observed temperature conditions, with 0.9% average error between predicted and observed bottom temperatures and 4.9% average error in surface temperatures.

Following grid development and model calibration and validation, LEAPS operation was incorporated into the model. LEAPS operation was assumed to proceed 5 days a week throughout the year, with flows during pumping and generation of 86.3 and 64.7 m³/s, respectively. Supplemental flows sufficient to maintain the lake level at approximately 1247' and 1240' were also provided. The preliminary intake specifications provided by Nevada Hydro included a 150 m wide shore-mounted structure with a bottom intake channel at 1220'. Simulations were conducted in which the intake was located at the Santa Rosa and Ortega Oaks sites on the west site of the lake. The effect of narrowed gate and slot widths were included in the assessment to evaluate selective withdrawal and delivery.

Model simulations demonstrated regular variations in the lake surface elevation associated with pumping and generation. Pumping that commenced at the end of the day Friday lowered the predicted lake level by a predicted 1.6 ft, before generation

during the weekdays incrementally increased the lake level by 0.8 ft while pumping subsequently decreased the lake level by about 0.6 ft per day, for a net daily increase of approximately 0.2 m/d during the week.

Velocities near the intake varied vertically and with increasing distance from the intake as a function of LEAPS operation, intake configuration and lake surface elevation. LEAPS operated near the nominal maximum operational surface elevation of 1247' yielded predicted velocities during generation near the intake averaged about 3.9 cm/s at the Santa Rosa site and 4.1 cm/s at the Ortega Oaks site. Somewhat higher velocities were predicted near the intake during pumping (5.2 - 5.3 cm/s). Predicted velocities were slower near the sediments than higher in the water column due to frictional losses at the sediment-water interface. Velocities also generally increased out about 100 - 140 m from the intake as flows were forced over a shallow sill formed from excavation and construction of the intake structure. Velocities slowed at greater distances from the intake, with little effect of LEAPS on velocities found beyond 500 - 600 m from the intake. Velocities exerted a shear force on the bottom sediment, although the magnitude of the bottom shear near the intake (on the order of 0.01 - 0.02 N m⁻²) was well below the critical threshold for resuspension of 0.1 N m⁻². As a result, LEAPS operation at 1247' was not predicted to induce significant sediment resuspension. The additional turbulent kinetic energy inputs to the lake from pumping-generation were also predicted to have only small impact on stratification and mixing in the lake. LEAPS operation at the Santa Rosa site lowered the thermal gradient (ΔT) between surface and bottom waters by about 1.2 °C in late May, reduced the number of days where the lake was at least weakly stratified ($\Delta T > 1$ °C at 6 a.m.) by 11 (from 121 to 110 days over the course of the simulation year), but overall had no substantive impact on stratification in the lake. Operation at the Ortega Oaks site had even less of an effect (e.g., lowering ΔT in late May by <0.5 °C and reducing the number of days where ΔT exceeded 1 °C by 5 days). The number of days in the simulation year with strong stratification ($\Delta T > 3$ °C) was minimally affected (51 days under natural conditions vs. 48 and 51 days for LEAPS operation at the Santa Rosa and Ortega Oaks sites, respectively).

Velocities and bottom shear production near the intake increased at the nominal minimum operational lake level of 1240', although predicted bottom shear remained below the critical value for resuspension. The lower lake level (without LEAPS operation) reduced the number of days of strong stratification from 51 at 1247' to 38 days at 1240'; thus, declining lake level had more dramatic of an effect than LEAPS operation at 1247',

where 48 and 51 days of strong stratification were predicted for the Santa Rosa and Ortega Oaks sites. The average duration of stratification was also reduced, from 8.5 days at 1247' to 6.3 days at 1240'. LEAPS operation at 1240' lowered the number of days of strong stratification from 38 (without LEAPS) to 33 and 35 days for the 2 intakes, although no effect on the average duration of stratification was predicted. Thus, even at this lower lake level, LEAPS was not found to alter, in either beneficial or negative ways, water column properties in the lake when the full cross-sectional area of intake conveyed flow.

Additional simulations were also conducted at 1247' to evaluate the potential for selective withdrawal-return to alter water column properties. The selective withdrawal of water during pumping, combined with the focusing of return flows during generation, may weaken stratification and help maintain oxic conditions near the sediments more effectively than using the full cross-sectional area of the intake for flow. Simulations found no significant effect of selective withdrawal-return through 1-m wide slot widths on stratification and mixing, while bottom release created areas of locally high bottom shear that ranged from 6 - 20 acres in size. The effect was quite dramatic as intake gate widths were narrowed from 150 m to 10 m, with local predicted suspended solids concentrations potentially exceeding 5000 mg/L for a 10 m x 1 m gate dimension at the Ortega Oaks site. The high level of local suspended solids would neither be chronic nor greatly affect lakewide suspended solids concentrations, however.

In summary then, the EFDC model predicted only small effects of LEAPS operation on water column properties in Lake Elsinore. This is thought to be the result of 2 factors. Most importantly, the proposed shore-based intake (at either site) is located a substantial distance from deep water, and is separated by a shallow sill that is approximately 2.7 – 5 m deep depending upon lake elevation. The local bottom topography near the intake thus limits efficient momentum flux to the deeper regions of the lake, and instead promotes local turbulence and short-circuiting of flow. Counter-current flow was in fact predicted under all selective withdrawal-return intake configurations. Moreover, this sill constrains the pumping of water from the warmer, upper portion of the water column. The 2nd factor thought to influence predicted results stems from the small net effect on water temperature of pumping, storage and generation (Anderson, 2006b). That is, the water is withdrawn and returned at comparable temperatures and densities so that buoyant forces are not expected to help focus flows to either surface and bottom depths in the lake.

1.0 Introduction

Operation of the Lake Elsinore Advanced Pumped Storage project (LEAPS) will result in significant volumes of water being transferred between the upper storage reservoir and Lake Elsinore on a daily basis during active pumping and generation. Previous calculations suggested that 3.9 – 13.9 % of the lake volume would be pumped each day at the nominal maximum and minimum operating levels of 1247' and 1240', respectively (Anderson, 2006a). The physical effects of this include regular exposure and inundation of shoreline sediments and potential for resuspension of bottom sediments, as well as changes in stratification and mixing (Anderson, 2006a). Sediment resuspension and alteration of stratification and mixing have been reported in some pumped-storage reservoirs (USBR, 1993; Potter et al., 1982).

Sediment resuspension is important since it can hasten the release of nutrients, increase oxygen demand in the water column, lower transparency, and alter the productivity and ecology of the lake. Enhanced turbulent kinetic energy inputs associated with LEAPS operation may also weaken stratification and enhance dissolved oxygen (DO) levels in the lake (Anderson, 2006a).

To better understand these potentially critical effects of LEAPS operation on the water column properties of Lake Elsinore, a 3-dimensional (3-D) hydrodynamic modeling study was undertaken. For this assessment, the Environmental Fluid Dynamics Code (EFDC) originally developed by Hamrick (1992) was used. The EFDC model has been used in over a hundred TMDL studies across the country and is included in the USEPA's TMDL Modeling Toolbox (USEPA, 2007).

2.0 EFDC Model

The EFDC model solves the 3-D, vertically hydrostatic, free surface, turbulent averaged equations of motion for a variable density fluid. The model uses a sigma (stretched) vertical coordinate system with a Cartesian or curvilinear horizontal coordinate grid.

For this study, a Cartesian 100 m x 100 m computational grid was constructed from available bathymetric data that yielded 1402 water cells (Fig. 1). The vertical dimension was represented with an 8-layer sigma vertical coordinate system (that is, each cell was divided into 8 horizontal layers irrespective of cell depth).

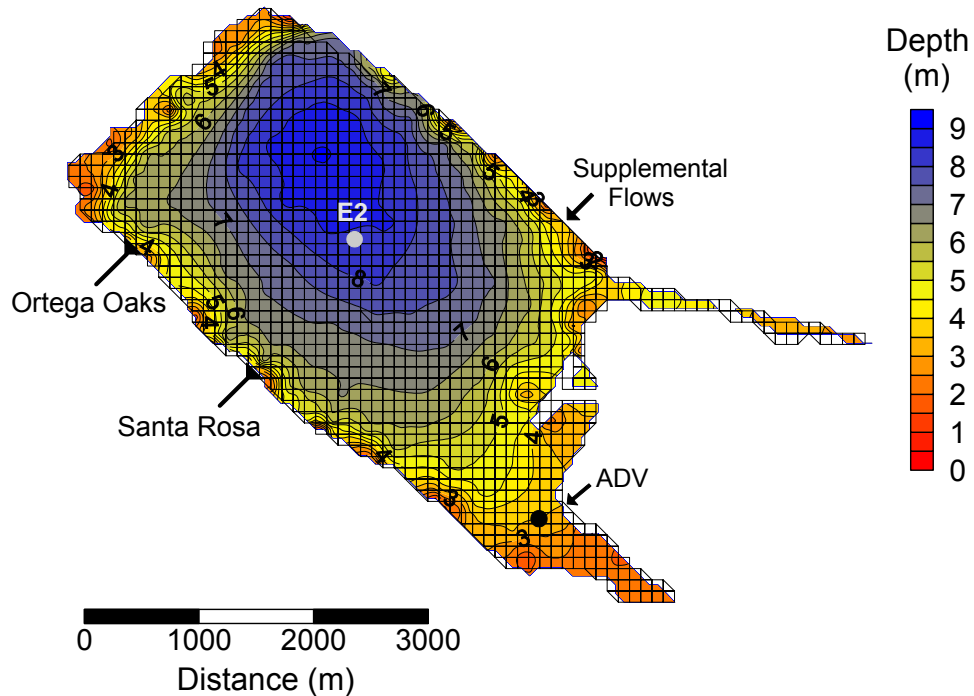


Fig. 1. Lake computational grid consisting of 1402 horizontal water cells and 8 vertical layers (not shown in this view). The bathymetry of the lake was developed from 293 depth soundings made in 16 transects across the lake in October 2006 and corrected to 1247' surface elevation. Site E2 is the water quality sampling station used for model calibration; the ADV site refers to the location of ADV velocity measurements made in August 2006.

The two proposed locations for the intake/outlet structure (referred to subsequently simply as the intake) for LEAPS was provided by Nevada Hydro. The two proposed sites for the intake are both located on the west side of the lake, with the Ortega Oaks site located in the north end of the lake, while the Santa Rosa site is near the middle of the western shore (Fig. 1).

2.1 Model Calibration

Following development of the computational grid, meteorological data were assembled and used with available water column data to calibrate the model. The period from March 1 – September 2006 was selected for model calibration since it represented at that time the current lake condition, was very close to the proposed upper operating range of LEAPS (1247'), and monitoring data (including temperature and velocity measurements) were available (Lawson and Anderson, 2006).

Air temperature, wind speed and wind direction data from a weather station a short distance away from the lake were provided by Elsinore Valley Municipal Water

District (EVMWD). Relative humidity, rainfall and solar radiation was taken from the California Irrigation Management Information System (CIMIS) meteorological station at UCR. Hourly data were used. Strong seasonal and diurnal changes in air temperature were observed (Fig. 2a). Marked diurnal variation in solar flux and wind speed were also observed (Fig. 2b,c).

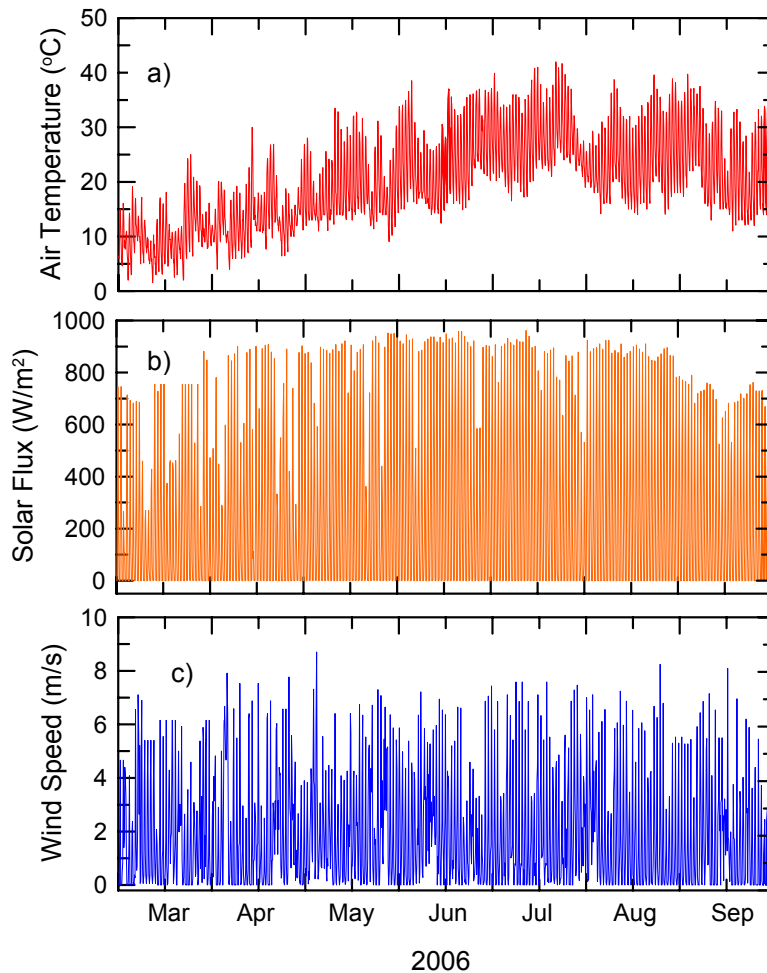


Fig. 2. Meteorological conditions used in the model calibration: a) air temperature, b) solar flux and c) wind speed.

With appropriate meteorological data to drive the model, the only water column property that also needed to be specified was the light attenuation coefficient; this coefficient was calculated from the average Secchi depth measured at the lake ($Z_{SD}=1.2$ m). Default values were used for all other parameters as specified in the model or taken

from a recent study of Lake Okeechobee (Jin et al., 2000). A 1-minute timestep was used in the model calibration process.

Using the default values, the model over-predicted daytime surface temperatures by 2 – 3 °C through much of the summer and under-predicted evaporative losses (data not shown). This suggested that the evaporative (and thus also convective) heat flux constants were too low. These two constants, which have the same numerical value in most applications, were thus varied to calibrate the model. Reasonable agreement between predicted (lines) and observed water column temperatures (symbols) was achieved when these two constants were increased from values of 1.5 to 2.0 (Fig. 3). The model captured the seasonal trend of strong heating of the both the surface and bottom waters beginning in the spring, predicting stratification over the period from May – June (with mixing events not captured in the biweekly field sampling) and mixing of the water column at the end of July (Fig. 3).

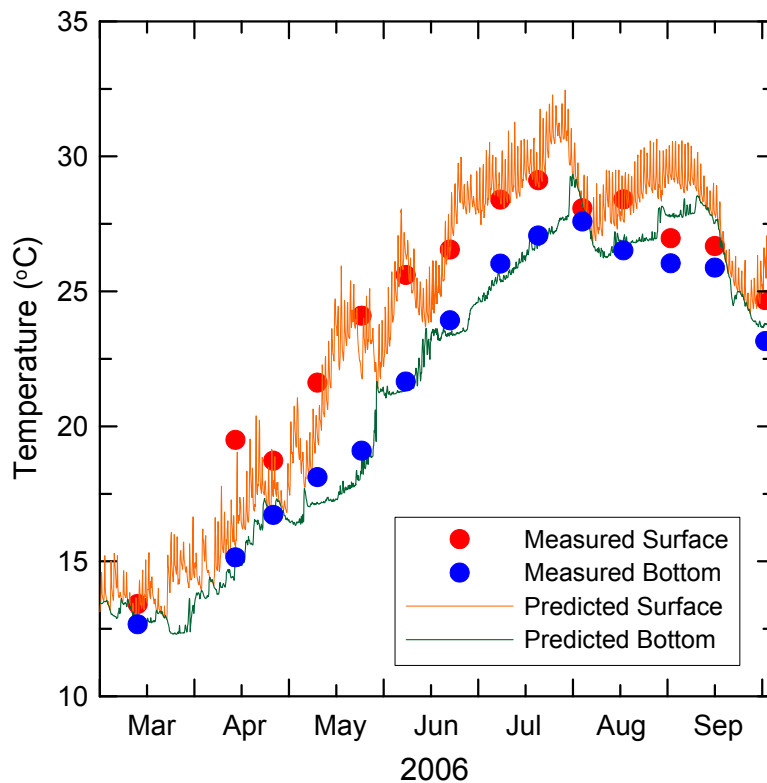


Fig. 3. Predicted and observed surface and bottom water temperatures at site E2 near the center of the lake (Fig. 1).

The model did over-predict temperatures in late August compared with observed surface and bottom temperatures, but reasonably reproduced temperatures in September (Fig. 3). The model also reasonably reproduced observed temperature

profiles at the main lake sampling station on most dates (e.g., Fig. 4). For example, the model quite accurately captured the temperature profiles measured on April 25th and May 23rd, including the late morning surface temperatures and diurnal thermocline that is typically present in the uppermost 1 m, as well as the thermocline that was present at 7-8 m depth (Fig. 4). While the model generally predicted temperature profiles in very good agreement with measured profiles, the model did over-predict temperatures in the upper 6 m of the water column on July 18th, although the predicted trend in temperature was similar to that observed (Fig. 4, Jul 18). The model also correctly predicted isothermal conditions on August 1st, and was within about 0.4 °C of the measured values.

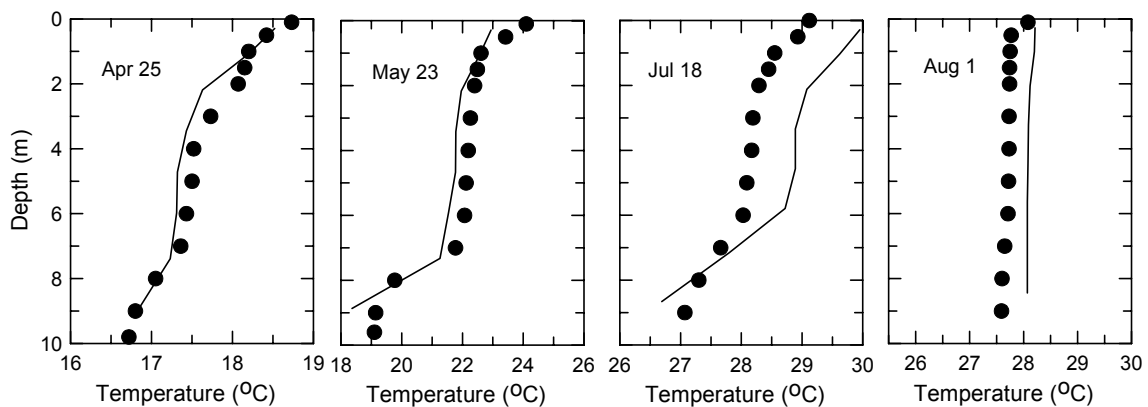


Fig. 4. Predicted (lines) and observed temperature profiles (circles) at site E2 near the center of the lake (Fig.1).

Measurements of bottom temperatures and water velocities made in the latter part of July in the shallow embayment in the southwest corner of the lake (Fig. 1, ADV site) were also used to assess the capacity of the model to reproduce conditions away from the central portion of the lake. This represents a rigorous test of the model since it includes both temperature and water velocities measured every 30 min in a shallow embayment that is subject to convective currents due to differential heating as well as advective currents which result from strong afternoon winds that blow from the northwest and into this embayment. The model predicted temperatures of 29-30 °C about 50 cm off of the bottom sediments, in good agreement with measured values (Fig. 5a, red line), especially when one recognizes that the initial conditions were specified almost 150 days prior. The acoustic Doppler velocimeter (ADV) recorded temperature (and velocity) every 30 min and thus allows a comparison of the diurnal variations in these properties with those predicted by the model (Fig. 5, inset). As one can see, the model also

reasonably reproduced the diurnal trends in temperature, increasing sharply in the afternoons of July 26-28 while being rather muted on July 25th (Fig. 5, inset). The model did underpredict the magnitude of these diurnal spikes in temperature associated with the downward mixing of warm surface layers due to the afternoon winds, but over this interval the average predicted temperature of 29.62 °C was only 0.62 °C higher than the average measured value of 28.98 °C (2.2 % error). The observed differences may be due in part to the slightly different depths for the measured and predicted values (approximately 50 cm and 25 cm off of the bottom, respectively).

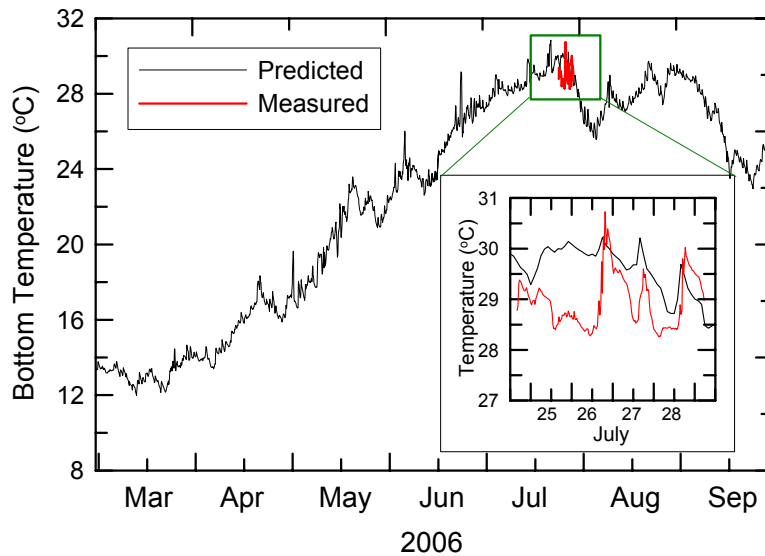


Fig. 5. Predicted and observed bottom water temperatures at the ADV site in the southwest corner of the lake (Fig. 1).

The ADV measures both the east and north components of the horizontal water velocity vectors and allows for ready comparison with the predicted velocity vectors from the EFDC model (Fig. 6). Negative values refer to components of the velocity vectors in the opposite direction (i.e., in the west and south directions). Measured velocities exhibited strong swings in direction and magnitude, with currents above the sediments and near the mouth of the embayment directed in the southerly and westerly directions in the afternoon, and moving somewhat slower and to the north and east later in the day (Fig. 6). The model captured these swings in velocities reasonably well, but predicted quite a bit lower velocity magnitudes (Fig. 6). The disagreement in the magnitudes of velocity may also be a product of slightly different depths between that measured and predicted, especially since velocities can decrease exponentially near a surface.

Notwithstanding, this is considered to be adequate agreement between measured and predicted velocities given the rigor of this test.

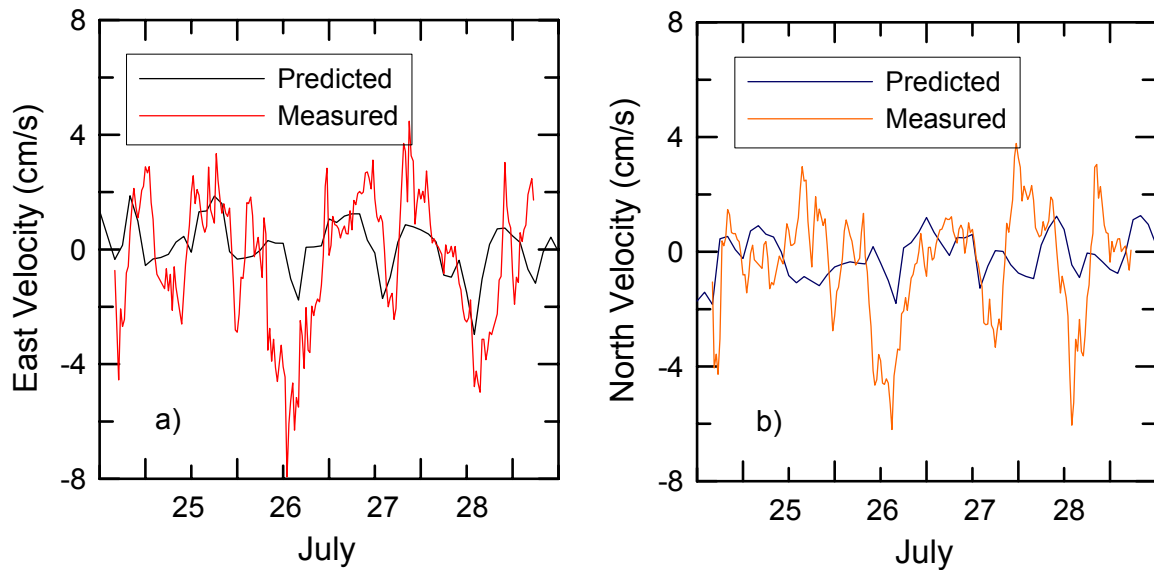


Fig. 6. Predicted and observed bottom water velocities at the ADV site (Fig. 1): a) east component of the velocity vector and b) north component of the velocity vector.

2.2 Model Verification

Following the model development and calibration described above, the next step was to verify the model using an independent data set. For model verification, a very different lake condition was selected. Specifically, 2001 was chosen since it represented a much lower lake level than that used for calibration (approximately 1241.5' lake surface elevation) and since a fairly extensive set of water column profile measurements were made (Anderson, 2001). The grid developed for 1247' was used as the starting condition for the lake on January 1. The lake was quickly brought down to approximately 1241.5' by withdrawing water from the lake at a rate of 51 m³/s over the next 7 days. The model was run through Julian day 180 (June 29th) for comparison with available temperature profiles. A 4-second timestep was necessary for this simulation due to the rapid drying of shallow regions of the lake.

All meteorological data were taken from a weather station deployed at the lake (rainfall, air temperature, relative humidity, wind speed, and wind direction) except solar radiation, which was taken from the CIMIS station at UCR as done in the model calibration phase described above. Simulations results were compared with high

resolution water column temperature data collected in May-June 2001 using 10 Onset temperature loggers deployed from 0.3 – 7.3 m depth near site E2.

Temperature loggers revealed an interval of strong stratification in early May that weakened through the month (Fig. 7a). The water column then mixed and warmed to approximately 26 °C in late June. Daytime surface temperatures often exceeded 28 °C (Fig. 7a).

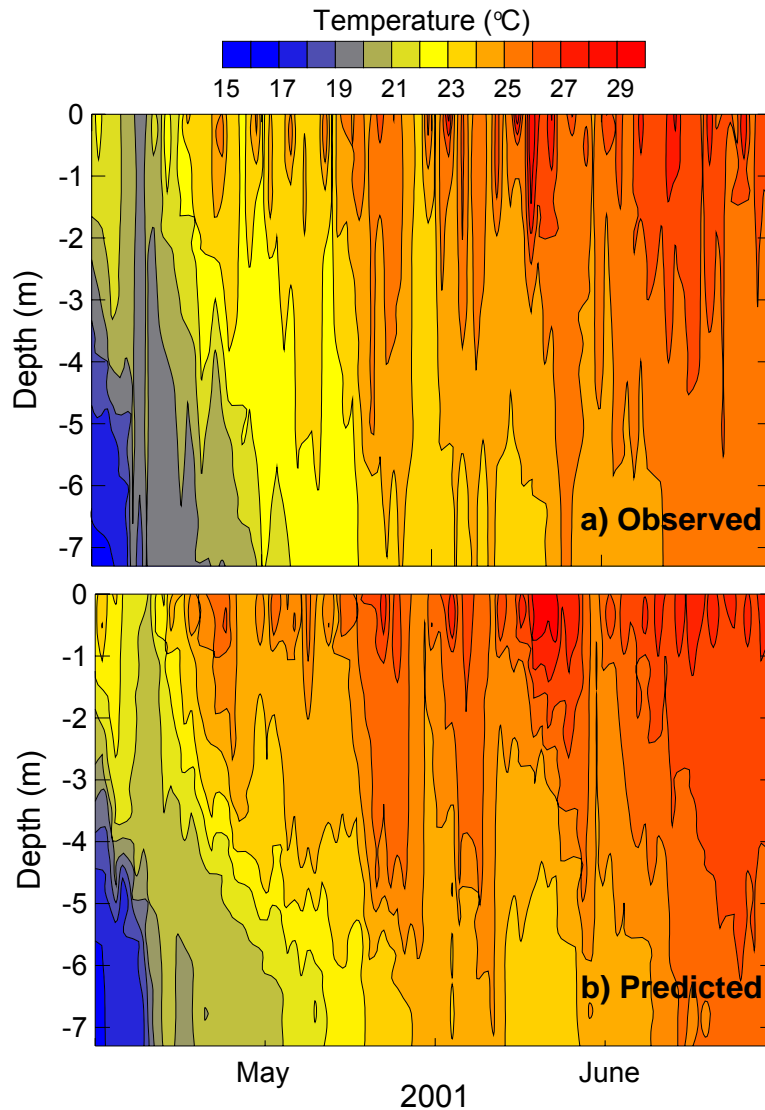


Fig. 7. Water column temperatures at site E2: a) observed and b) predicted temperature profiles over time.

The model reproduced quite satisfactorily the major features found in the measured temperature profiles during this period (Fig. 7b). That is, it predicted stratification in early May, with cool (~16 °C) temperatures present below about 5 m depth that increased to about 20 °C by mid-May (Fig. 7b). The model also predicted

intervals of somewhat weaker, transient stratification later in May and into June and temperatures exceeding 26 °C by late June.

Looking more carefully at the predicted and observed temperatures near the surface (about 0.3 m depth) and bottom (about 7 m depth), one sees that the model reasonably predicted the strong diurnal trends in surface temperatures as well as longer term trends, although slightly over-predicted their absolute values (Fig. 8). The model yielded predicted bottom temperatures in fair agreement with measured values as well.

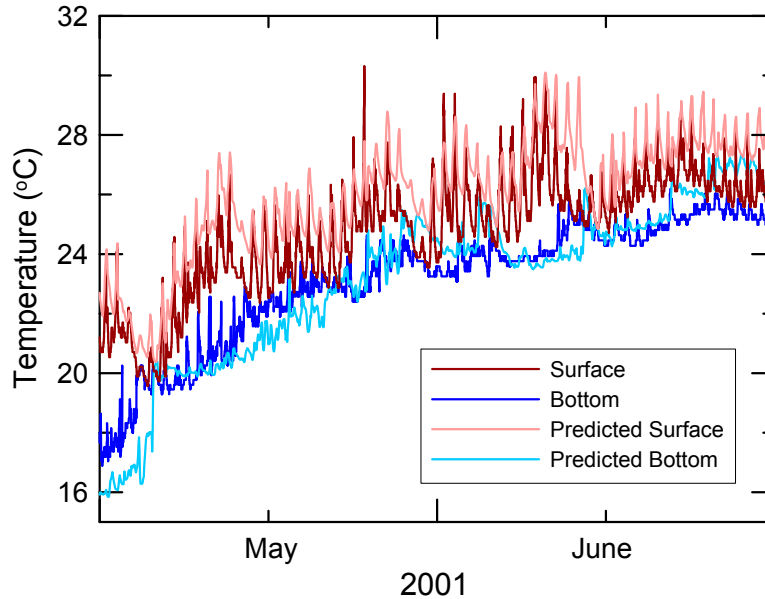


Fig. 8. Predicted and observed surface and bottom water temperatures at site E2.

The model did yield surface and bottom temperatures that consistently exceeded measured values (Table 1). The modeled surface temperature was on average 1.18 °C warmer than the measured values, while somewhat better agreement was found between the predicted and measured bottom temperatures (Table 1). The relative % error ($T_{\text{error}}/\text{measured temperature}$) averaged about 5% and 1% for the surface and bottom temperatures, respectively (Table 1).

Table 1. Error analysis for model validation (data shown in Fig. 8).		
	Surface	Bottom
T_{error} (°C) (Pred-Obsd)	1.18 ± 0.75	0.26 ± 0.79
Relative Error (%)	4.92 ± 3.09	0.94 ± .57

Based upon these findings, it may be that the evaporative and convective heat loss constants could be increased slightly higher to take a little more heat out of the surface of the lake. Notwithstanding, the overall very good agreement between predicted

and observed temperatures for both 2001 (low lake level) and 2006 (high lake level), as well as the adequate agreement with water velocity measurements made in 2006, indicates that the model should provide accurate and valuable insights in the effects of LEAPS operation on the physical properties of Lake Elsinore.

3.0 LEAPS Simulations

Simulations were conducted to represent a number of different design and operational scenarios. Two different sites (Fig. 1), and 2 different lake surface elevations (1247' and 1240' were evaluated. The Santa Rosa site has emerged as the preferred site, although simulations were also conducted for the Ortega Oaks site to explore the effect of intake location on lake circulation and mixing. The details of the intake structure are expected to have a potentially substantial effect on water column properties during operation. As a result, 4 different configurations were evaluated. In the 1st configuration, the full wetted cross-sectional area of the proposed 150 m wide intake structure was assumed to provide flow during pumping and generation. Alternative scenarios were also investigated in which the intake dimensions were varied from 150 m wide to gate widths of 40 and 10 m. Horne (2005) suggested that the elevation of intake and discharge may also be used to advantage, e.g., to preferentially entrain buoyant blue-green algae and also enhance DO conditions near the bottom sediments. As a result, the effect of discharge elevation was also investigated in some detail for the two sites.

Before these simulations were conducted, however, some additional information was added to the model

3.1 Flows

Two different sets of flows were added to the model. The first was supplemental water proposed to be added to help stabilize the lake level (Nevada Hydro, 2005). Water was added at the outlet channel previously used in a pilot project to help stabilize lake level with recycled water provided by EVMWD (Fig. 1). Based upon historical data about observed declines in lake level, supplemental water was added to the lake from April through November. Rainfall and runoff in amounts that are not known *a priori* make it difficult to forecast suitable supplemental flows during the winter, so no water was added from December – March (Fig. 9). Using predicted changes in lake surface elevation from previously described simulations, supplemental water was added at rates up to 1 m³/s (Fig. 9).

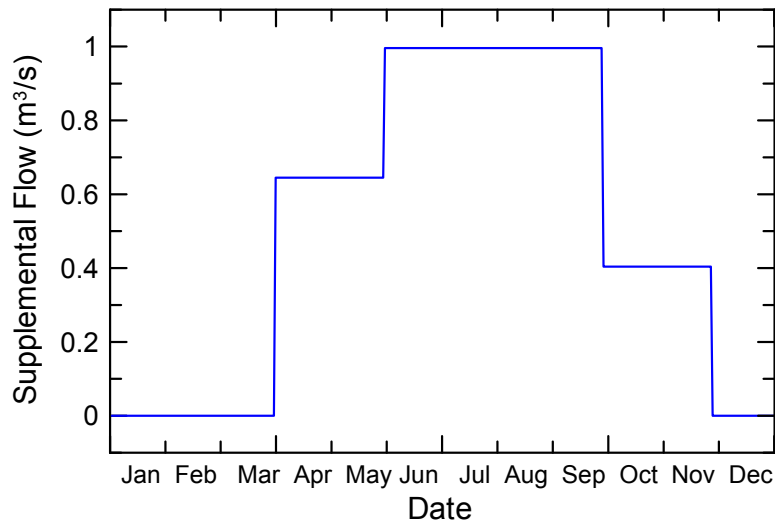


Fig. 9. Supplemental flows to Lake Elsinore to maintain lake elevation.

Flows associated with LEAPS operation were varied regularly, with 5 days of generation (Monday-Friday) on a schedule with 7 hours of pumping and 15 hours of generation per day during the week (Fig. 10). Pumping proceeded for 21 h on Saturday to restore the net drawdown that occurred during the week as a result of daily generation flows exceeding that of pumping. Operation was assumed throughout the year.

3.2 Intake Structure Design

Intake specifications were provided by Nevada Hydro (R. Wait, pers. comm.) and included:

- overall shore structure approximately 42 ft high x 500 ft long
- elevation of intake channel at 1220 ft
- bottom elevation of intake gate at 1223 ft
- excavation out approximately 200 ft from intake to recontour bottom to slope to 1220 ft and place rip rap

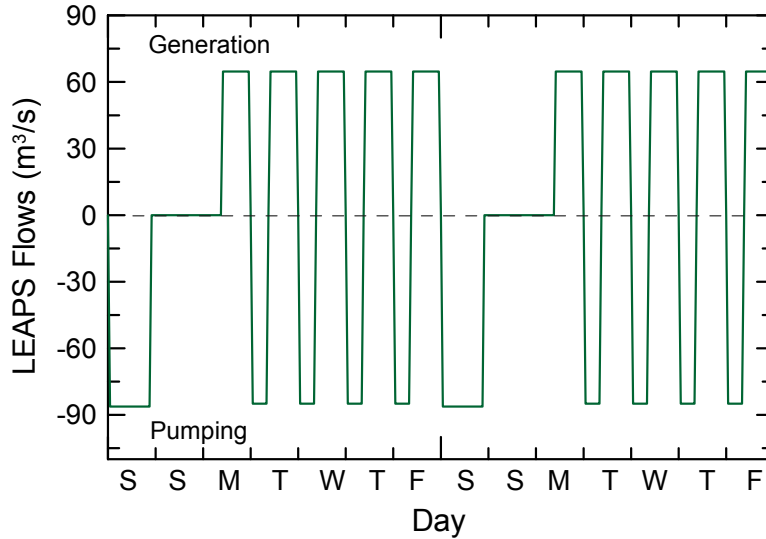


Fig. 10. Withdrawal and return flows due to LEAPS operation. This weekly pumping schedule was applied through the year.

The intake structure was placed at the existing 1240 ft bottom contour at the proposed Santa Rosa site (Fig. 1). Using available bathymetric data, it is proposed that the Santa Rosa site will look something like that shown in Fig. 11. The existing bottom contour out to 600 m perpendicular to the intake is shown, as well as the region that would require excavation (Fig. 11, shaded area). Based upon very limited depth soundings in this region, it appears that about 24,000 m³ of sediment would have to be removed to complete this design. Detailed surveying in the region is needed to more accurately estimate excavation requirements and final bottom contours.

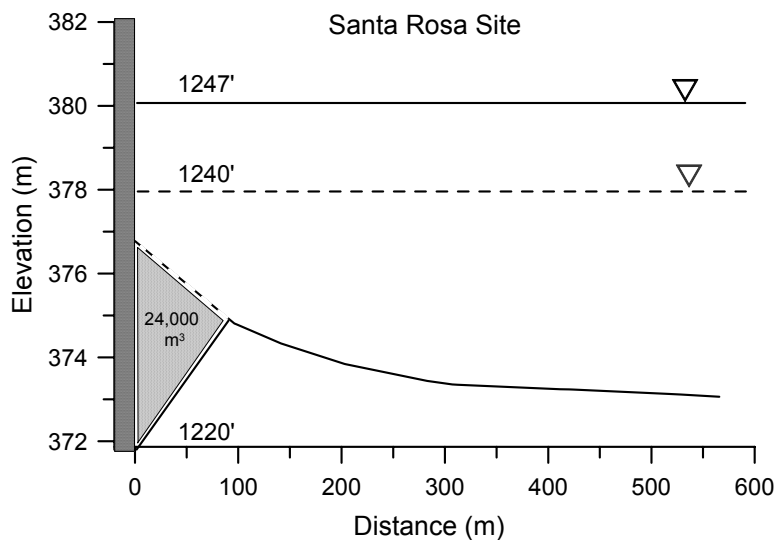


Fig. 11. Approximate longitudinal cross-section near intake showing bottom contour and zone of sediment excavation: Santa Rosa site.

Available bathymetric data and specific assumptions about placement of the intake suggest that the Ortega Oaks site (Fig. 1) is located in slightly shallower water, although the cross-section is very similar to that of the Santa Rosa site (Fig. 12). As a result, slightly more material would need to be excavated (an estimated 26,000 m³).

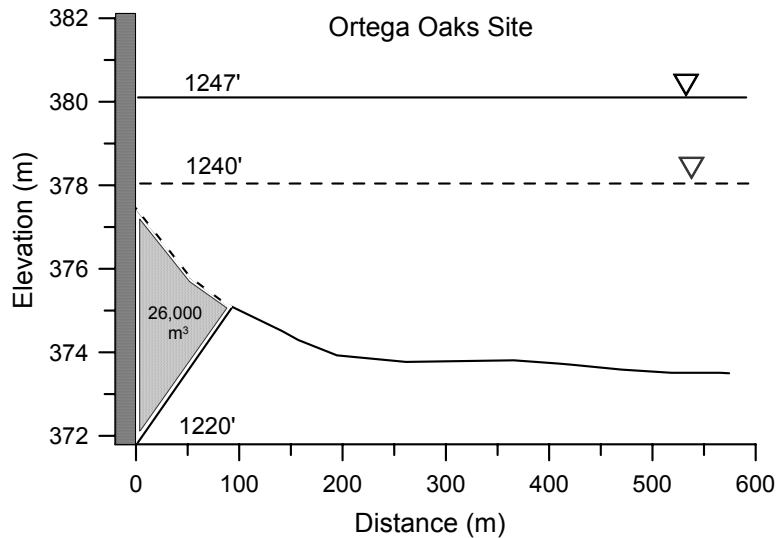


Fig. 12. Approximate longitudinal cross-section near intake showing bottom contour and zone of sediment excavation: Ortega Oaks site.

Flow at the intake structures was simulated using the standard river-type flow boundary condition for simulations assuming the full cross-sectional area of the structure delivers flow, while the withdrawal-return subroutine of the EFDC was used to simulate selective withdrawal and return flows at specific depths. Momentum flux was specified at the lake side of the intake structure following Hamrick (pers. comm.). For these latter simulations, withdrawal (pumping) removed water from the 4th layer (out of 8) for the 1247' scenarios, reflecting withdrawal through a 150 m x 1 m gate for the proposed intake design. To make the computational layers a comparable thickness at the intake at the 1240' surface elevation, 6 vertical layers with withdrawal at the 3rd layer (out of 6 total) were used. The effect of varying width of the intake-outlet structure was also evaluated (widths of 40 m and 10 m were used in these simulations).

4.0 Simulation Results

4.1 Lake Surface Elevation Changes During Operation

The pumping-generation scheme of LEAPS (Fig. 10) resulted in regular oscillation in the lake surface elevation (Fig. 13). The maximal lake elevation occurs at the end of the day Friday; the lake level then experiences its greatest daily decline as pumping through the day on Saturday was predicted to lower the lake level by 1.6 ft (Fig. 13), in good agreement with previous estimates of 1.7 ft (TNHC, 2004). Since no pumping was simulated for Sunday and early Monday, the lake level remained low until generation began near the start of the work day (Fig. 10). Generation through the day and into the early evening increased the lake level by about 0.8 ft, before pumping initiated at midnight began to lower the predicted lake level. Since daily volumes released during generation exceeded the amount of water pumped, lake levels increased incrementally each day through the week until, by the end of the day Friday, the cycle repeats (Fig. 13). While these results were predicted assuming a nominal lake level of 1247 ft, only modest differences would be expected at other lake levels (e.g., slightly greater daily and weekly oscillations in surface elevation).

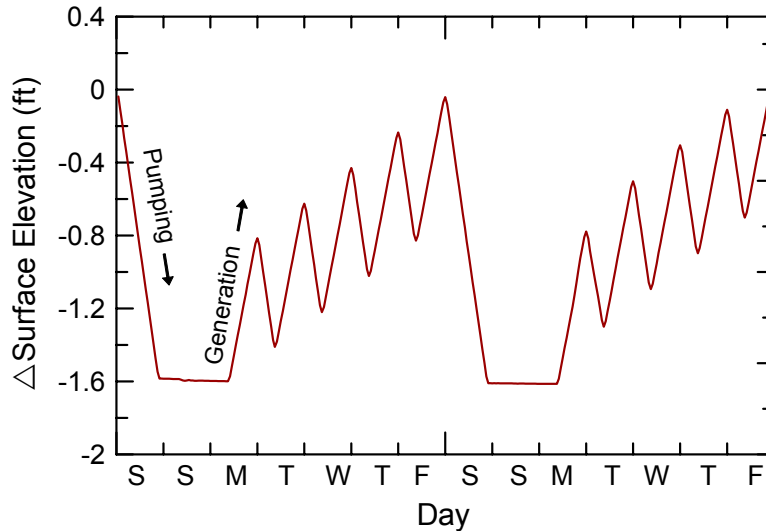


Fig. 13. Predicted elevation changes for Lake Elsinore during LEAPS operation (assuming a nominal surface elevation of 1247 ft and the pumping routine depicted in Fig. 10).

4.2 Velocities Near Intake

The pumping and generation phases of operation move significant volumes of water each day; plant operation can thus be expected to induce potentially strong currents near the intake. The velocity field perpendicular to the face of the intake varied

depending upon phase (pumping or generation), as well as the cross-sectional area for flow, and depth of withdrawal and return flows. In this section, predicted velocities near the intake will be presented for the operational scenario where the full wetted cross-sectional area of the intake (Figs. 11 and 12) conveys flow. The effects of selective withdrawal will be discussed in section 4.5.

4.2.1 Predicted Velocities Near Intake at 1247 ft

The EFDC model predicted a relatively uniform vertical velocity profile adjacent to the intake at the Santa Rosa site, although boundary layer effects slow the velocities above the sediments (Fig. 14). During pumping, an average velocity of 5.2 cm/s directed toward the intake was predicted near its face, with slightly higher velocities predicted closer to the surface (up to 6.2 cm/s at the uppermost simulation layer), and lower predicted velocities near the sediments (3.1 cm/s) (Fig. 14a). Velocities decayed at increasing distance from the intake, to a depth-averaged value of 3.7 cm/s at 140 m, 1.2 cm/s at 280 m and 0.6 cm/s about 420 m away (Fig. 14a).

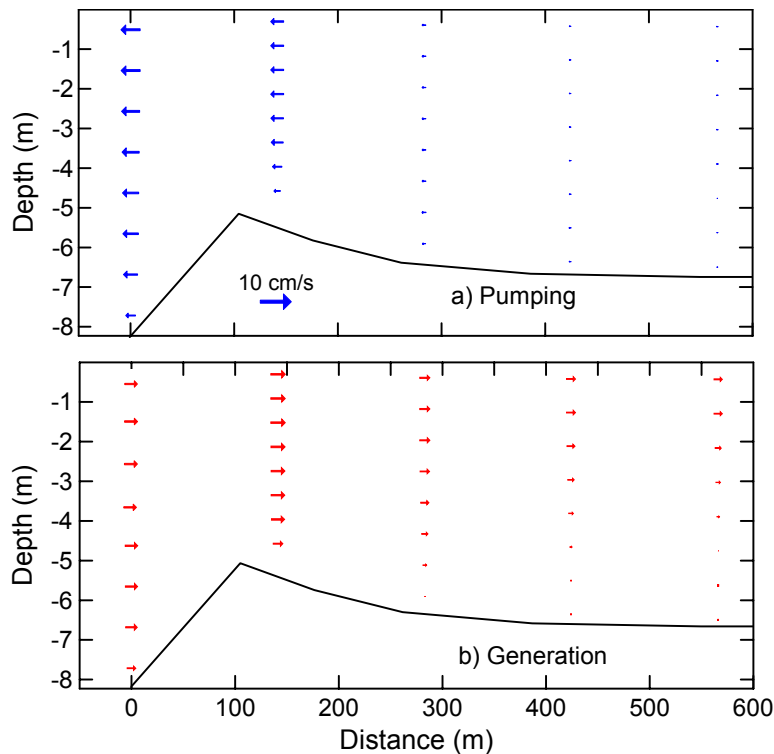


Fig. 14. Predicted velocity field perpendicular to the intake at the Santa Rosa site at 1247': a) pumping and b) generation. Active intake dimensions 150 m x 8 m with reversible flow across the full wetted cross-sectional area of the intake. Note reference velocity scale in upper panel.

The direction of flow reversed during generation, with lower velocities than found during pumping, reflecting the lower volumetric flow rates during generation when compared with pumping (Fig. 10). Velocities were somewhat lower near the sediments than found closer to the lake surface (e.g., 2.76 cm/s in the lowest simulation layer compared with 4.18 cm/s 1.5 m below the surface near the intake) (Fig. 14b). Vertically-averaged velocities increased from 3.87 cm/s near the intake to 4.34 cm/s at 140 m due to the shallower depth there, and then declined to average values of 2.34, 1.54 and 1.09 cm/s at increasing distances (Fig. 14b).

For comparison, predicted velocities near the intake during periods of non-operation averaged approximately 0.2 cm/s during intervals of comparatively low winds, although velocities exceeding 1 cm/s are often present during the afternoon when strong winds are often found. Thus, the demonstrable effects of LEAPS operation on the local velocity field under this operational scenario are predicted to extend out about 500 - 600 m from the intake.

The effect of locating the intake at the Ortega Oaks site was also evaluated, with the same set of meteorological and hydrological conditions as used in the Santa Rosa simulations to drive the model. The Ortega Oaks site differed from the Santa Rosa site in its location relative to the center of the lake as well as its local bathymetry (Fig. 1). Specifically, the Ortega Oaks site is shallower both in its longitudinal profile away from the intake (Fig. 12), as well as laterally (Fig. 1). At any given distance away from the proposed intake, the Ortega Oaks site is 2-9 % shallower than the Santa Rosa site. These relatively modest differences in local bottom contours and position on the lake may nonetheless potentially alter the lake response to the operation of LEAPS.

Assuming the full wetted cross-sectional area of the intake is available for flow, the EFDC model predicted velocities during pumping that were rather slow in the deepest layers adjacent to the intake (2.93 cm/s) and increased towards the lake surface (to values of 6.21 cm/s). The velocities at all depths increased out approximately 140 m from the intake to values of 3.46-6.05 cm/s and then slowed quite substantially at greater distances (Fig. 15a). Slightly slower velocities directed away from the intake and into the lake were predicted at any give depth and distance from the intake during generation (e.g., 2.77 – 4.42 cm/s adjacent to the intake) (Fig. 15b), velocities that were slightly faster than found at the Santa Rosa site (Fig. 14b).

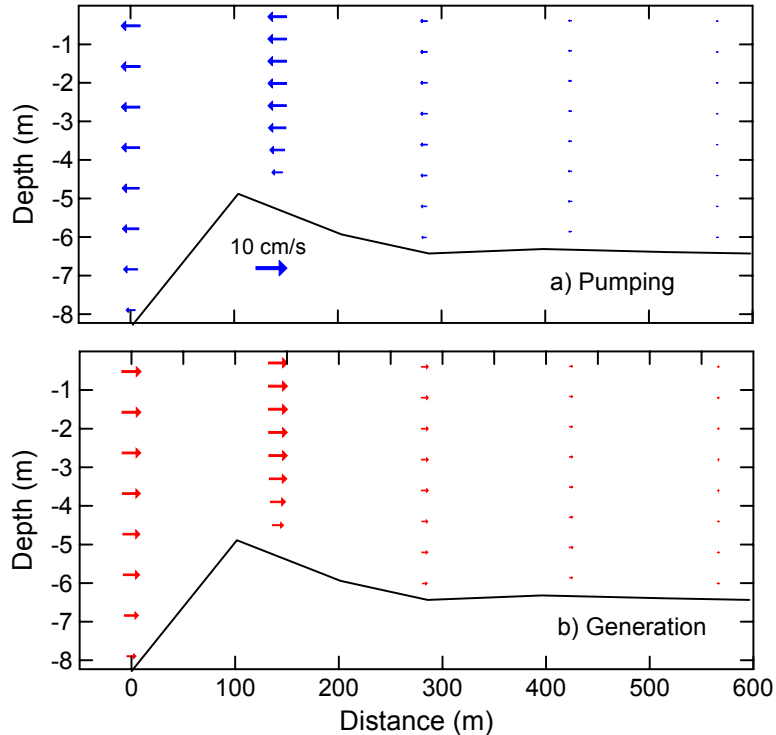


Fig. 15. Predicted velocity field perpendicular to the intake at the Ortega Oaks site at 1247': a) pumping and b) generation. Active intake dimensions 150 m x 8 m with reversible flow across the full wetted cross-sectional area of the intake. Note reference velocity scale in upper panel.

4.2.2 Predicted Velocities Near Intake at 1240 ft

The lower lake level functionally reduces the intake cross-sectional area available for flow, so one would expect greater velocities under these conditions. The lowered lake level in fact had a significant effect on velocities near the intake (e.g., compare Fig. 16 with Fig. 14). Velocities adjacent to the intake at the Santa Rosa site during both pumping and generation (Fig. 16) were on average 1.45x higher than the velocities predicted during pumping when the lake level was at 1247' (Fig. 14). This increase is due in large measure to the smaller depth and thus lower cross-sectional area available for flow, although increased channeling of flow due to the lower depths of neighboring regions of the lake also appears to have increased flow velocities perpendicular to the face of the intake. This can be seen when one considers that, based only on cross-sectional areas, one would expect an increase of about 1.35x, while velocities adjacent to the intake increased by a larger amount, to 3-4 cm/s near the sediment and greater than 9 cm/s near the lake surface. High velocities were also present 140 m from the intake as flow was squeezed into a smaller depth, but declined at further distances as the water deepened (Fig. 16).

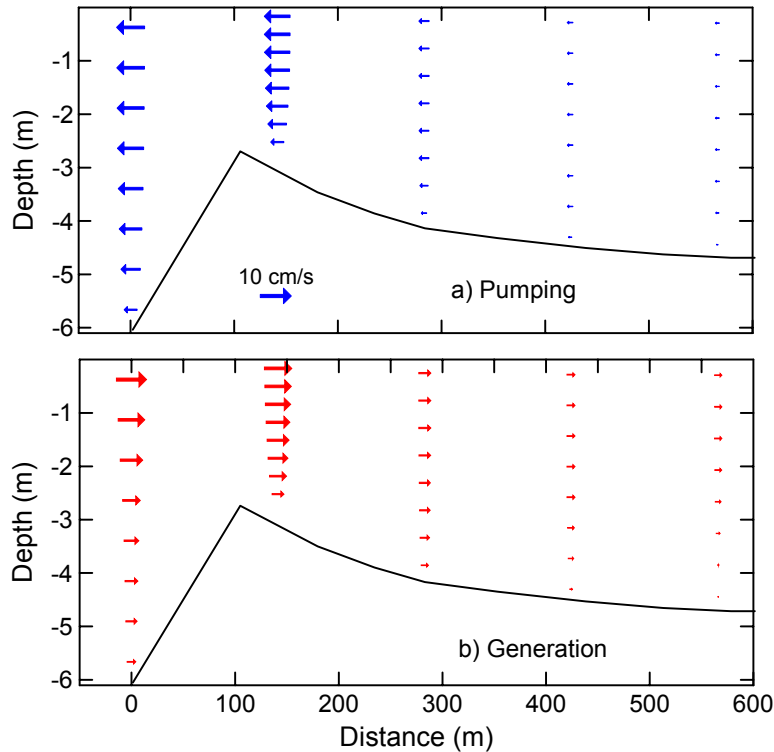


Fig. 16. Predicted velocity field perpendicular to the intake at the Santa Rosa site at 1240': a) pumping and b) generation. Active intake dimensions 150 m x 6 m with reversible flow across the full wetted cross-sectional area of the intake. Note reference velocity scale in upper panel.

The 1240' elevation had more pronounced of an effect on the predicted velocity profiles at the Ortega Oaks site than predicted for the 1247' surface elevation, especially 140 m from the intake where the velocities reached 13 cm/s during pumping and exceeded 11 cm/s during generation (Fig. 17). Higher velocities were also predicted at greater distances from the intake, and on average were 1.5x higher than observed at 1247'.

At an equivalent lake elevation of 1240', the two sites also differed in their relative velocities. The Ortega Oaks site yielded velocities that were, on average, 1.4x higher during pumping and 1.2x higher during generation than predicted for the Santa Rosa site.

Water velocities near the intake are important since they influence turbulent kinetic energy inputs to the water column that can alter stratification and mixing in the lake, as well as lead to sediment resuspension, entrainment, and other processes. We turn our attention now to the potential for LEAPS operation to resuspend bottom sediments and thus alter turbidity, dissolved oxygen and nutrient levels in the lake.

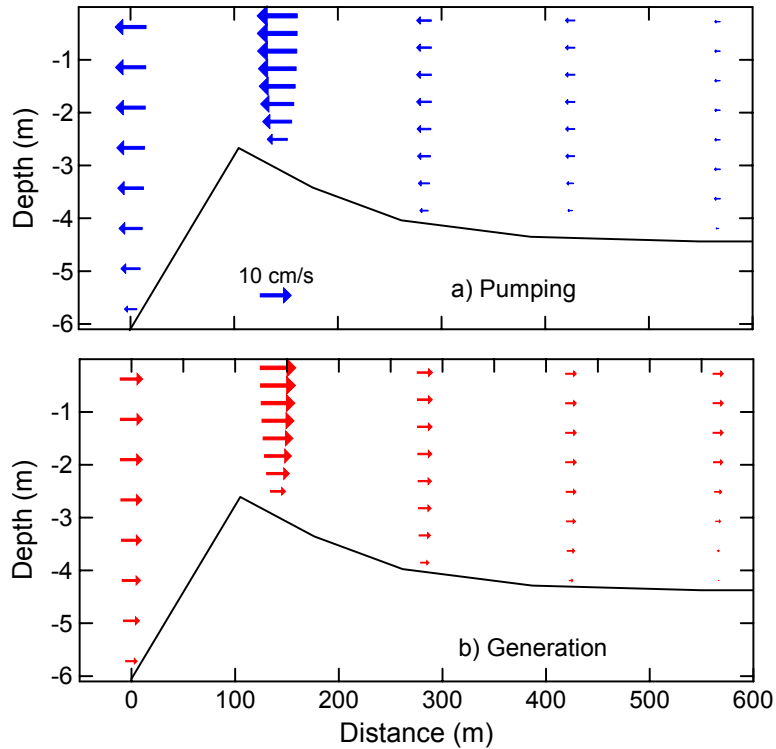


Fig. 17. Predicted velocity field perpendicular to the intake at the Ortega Oaks site at 1240': a) pumping and b) generation. Active intake dimensions 150 m x 6 m with reversible flow across the full wetted cross-sectional area of the intake. Note reference velocity scale in upper panel.

4.3 Bottom Shear and Sediment Resuspension

4.3.1 Predicted Bottom Shear at 1247 ft

Water flowing over the sediment surface creates a shear stress (τ) that can potentially resuspend bottom sediments. Specifically, resuspension occurs when τ exceeds a critical shear stress (i.e., when $\tau > \tau_c$). Typical values for τ_c are 0.1-0.2 N m⁻² (Chapra, 1997). In a study of sediment resuspension in Lake Okeechobee, Ji and Jin (2005) used a critical shear stress value of 0.18 N m⁻². For this analysis, I assumed a τ_c of 0.1 N m⁻². For reference, the average afternoon bottom shear across the lake was about 0.004 N m⁻² from simulations without LEAPS operation, although values exceeding 0.1 N m⁻² can be found in shallow regions of the lake during high winds.

The mass of sediments scoured from the bottom (ε) can be calculated from bottom shear by (Chapra, 1997):

$$\varepsilon = \frac{\alpha_0}{t_d^2} (\tau - \tau_c)^3 \quad (1)$$

where α_0 and t_d are constants. Importantly, one notes that ε increases as the cube of the difference between bottom shear and the critical shear; thus an increase in bottom shear will result in an exponential increase in mass of sediment scoured. Studies have shown that the entrainment of bottom sediments at a given shear stress occurs over a period of about an hour, with no additional entrainment occurring unless shear stress is increased (Chapra, 1997). That is, the sediment comes into equilibrium with the local energy environment relatively quickly, thus resuspension is expected only during transition periods when shear increases. The concentration of suspended solids (C_{ss}) can be estimated from ε and the depth of the water column (H) from:

$$C_{ss} = \frac{\varepsilon}{H} \quad (2)$$

Predicted bottom shear during pumping and generation across the intake at 1247 ft surface elevation (velocity field depicted in Fig. 14) indicate that levels higher than typical background levels were restricted to relatively small areas proximal to the Santa Rosa site, although the values were below critical shear values that would result in sediment resuspension (Fig. 18). Shear stress reached maximum values of only about 0.02 N m^{-2} adjacent to the intake during pumping and 0.01 N m^{-2} during generation, and decreased quickly with distance. This is consistent with velocity profiles that showed that bottom velocities decreased rather strongly within a few hundred meters of the intake (Fig. 14).

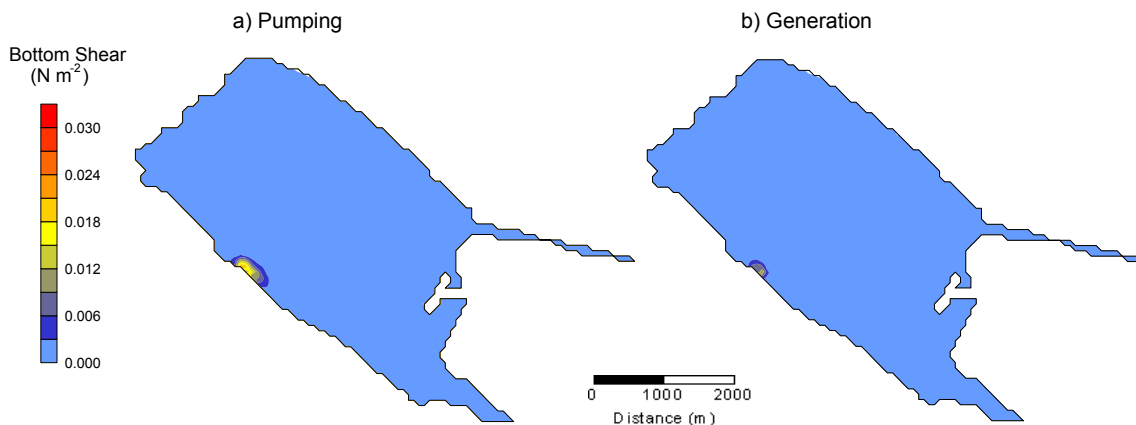


Fig. 18. Predicted bottom shear at the Santa Rosa site at 1247 ft lake surface elevation.

Importantly then, predicted bottom shear remained below the critical value of 0.1 N m^{-2} (Fig. 18), so LEAPS operation in this configuration is not expected to resuspend bottom sediments (the area immediately in front of the intake is excluded since rip-rap placed there is not considered a significant source of resuspended sediment).

Similar to that predicted from the Santa Rosa site, predicted bottom shear at the Ortega Oaks site during pumping and generation phases indicate that levels higher than typical background shear levels were restricted to relatively small areas proximal to the intake (Fig. 19). Under this operational scenario, in which the full width and height of the intake was used during pumping and generation, bottom shear values at the Ortega Oaks site also remained below the assumed critical value of 0.1 N m^{-2} and fell quickly away from the intake (Fig. 19).

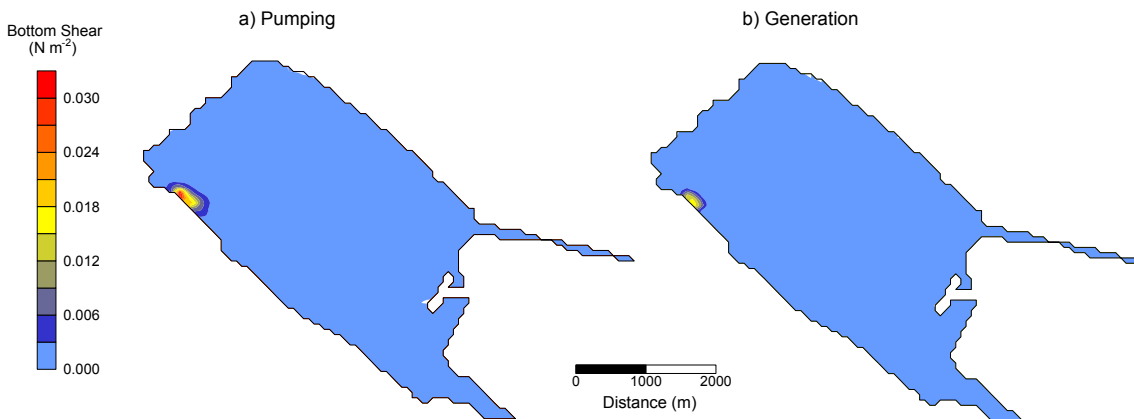


Fig. 19. Predicted bottom shear at the Ortega Oaks site (1247 ft lake surface elevation).

4.3.2 Predicted Bottom Shear at 1240 ft

Operation of LEAPS at the nominal minimal lake elevation of 1240 ft was previously shown to increase the velocities near the intake due to the lower effective cross-sectional area available for flow (e.g., Figs. 15 and 17). Since bottom shear increases with increasing velocity, one expects greater bottom shear and potential for sediment resuspension at lower lake levels. This is borne out in model predictions, where higher values of bottom shear and larger overall areas of elevated bottom shear were found at both the Santa Rosa and Ortega Oaks sites (e.g., Fig. 20) relative to those found at 1247 ft surface elevation (Fig. 18b, 19b). Note that the results in Fig. 20 are for

the generation phase of LEAPS operation, where resuspended sediment would potentially lower light transparency and increase nutrients in Lake Elsinore.

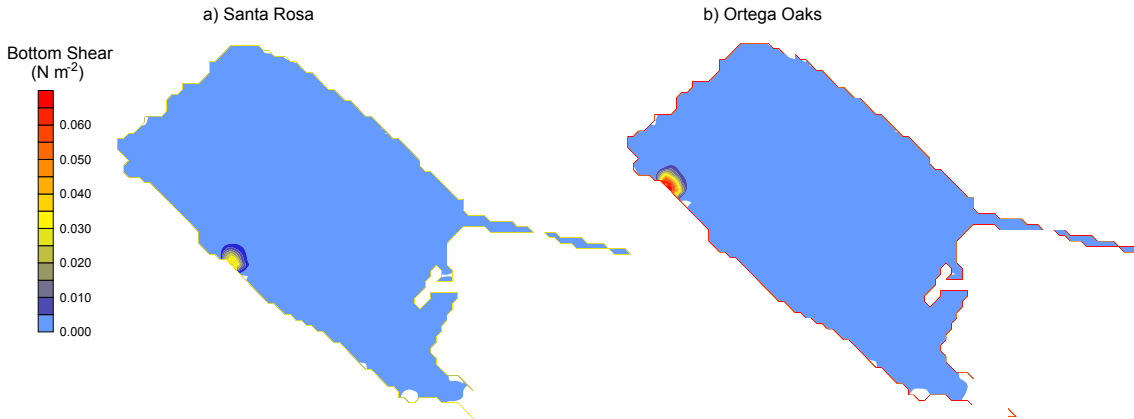


Fig. 20. Predicted bottom shear during generation at the a) Santa Rosa and b) Ortega Oaks site (1240 ft lake surface elevation).

Importantly, however, using the full face of the intake for withdrawal and return flows yielded predicted shear values that remained below levels expected to resuspend bottom sediments. Thus, even at a lake level of 1240', sediment resuspension is not expected to be a significant concern using the full wetted cross-sectional area of the intake. (The effect of selective withdrawal, especially bottom return flows, on sediment resuspension is greater, as will be discussed later in section 4.5.)

We now turn our attention to the influence on stratification and mixing of additional TKE inputs to the lake due to plant operation.

4.4 Effect on Stratification and Mixing

4.4.1 Stratification and Mixing at 1247 ft

The potential for the operation of LEAPS to alter stratification and mixing in the lake was also evaluated. The predicted thermal regime of the lake at 1247' without LEAPS operation (but with supplemental flows to maintain lake level) was similar to that seen previously as part of the model calibration and verification process. Cool, isothermal conditions were predicted for January and February, with strong stratification setting up in March (Fig. 21). Stratification in March has also been seen each spring in the lake monitoring we have conducted for the past several years. Surface waters were then predicted to cool, resulting in the weakening of stratification and mixing in April,

followed by subsequent surface heating to yield temperatures reaching about 28 °C in the summer (Fig. 21). The lake was then predicted to cool beginning in September, with isothermal conditions present through the fall when temperatures again returned to approximately 10-12 °C in December.

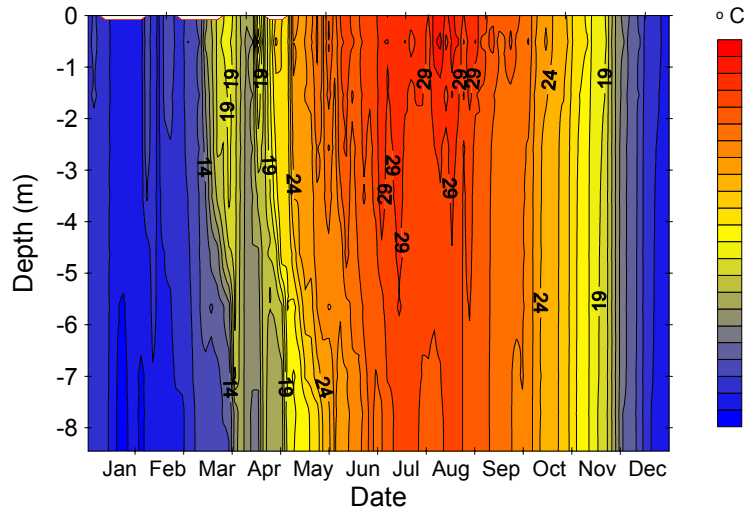


Fig. 21. Predicted water column temperatures at site E2 without LEAPS operation (1247 ft lake surface elevation).

The presence of thermal stratification can be seen more readily in Fig. 22, where ΔT values, taken here as the difference in temperatures at site E2 (Fig. 1) at the 2nd and 8th computational layers (corresponding to 1.2 and 7.6 m depths), are plotted over time. Low values of ΔT correspond to weak thermal stratification and indicate there is only a small and transient energy barrier to mixing; such a condition would generally indicate that dissolved oxygen (DO) levels would not decline strongly in the bottom waters, and NH_3 and H_2S concentrations would remain low. Strong stratification, on the other hand, would generally persist for longer periods of time and allow severe depletion of DO and accumulation of potentially high levels of reduced species in the lower water column.

Comparatively low predicted values of ΔT were generally present in January and February, although ΔT did briefly exceed 3°C in early February (Fig. 22). The lake strongly stratified in March, with ΔT exceeding 6 °C, but ΔT declined quickly with the water column mixing briefly in April, before restratifying later in April and May (Fig. 22). The intensity of stratification began to weaken in June, however, as the lake volume continued to warm (Fig. 21). Quite low values of ΔT were in place beginning in

September, with very low values from October to December indicating well-mixed conditions (Fig. 22).

These seasonal trends were in place for all 3 scenarios (the reference condition, in which LEAPS was not in operation, as well as during operation at the Santa Rosa and Ortega Oaks sites) (Fig. 22). It was in fact difficult to see the reference (no LEAPS) case on the figure, being obscured by the other lines, although it does appear that operation of LEAPS at the Santa Rosa site weakened slightly the strength of stratification relative to LEAPS operation at the Ortega Oaks site and at the reference condition (Fig. 22).

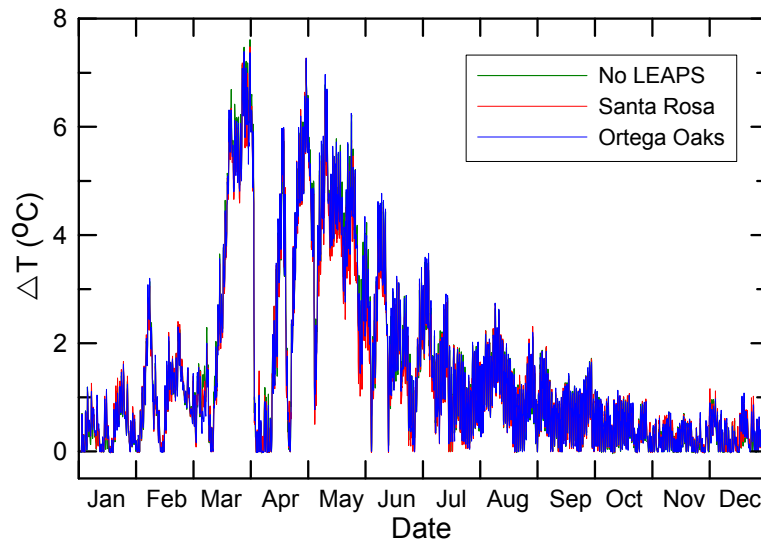


Fig. 22. Temperature differential (ΔT) between surface and bottom waters without LEAPS operation and operation at the Santa Rosa and Ortega Oaks sites, 1247 ft surface elevation.

To highlight more clearly the effects of LEAPS operation on the strength of stratification, the ΔT values calculated for the Santa Rosa and Ortega Oaks sites were subtracted from the ΔT value at any given time predicted when LEAPS was not in operation (Fig. 23). If there was no effect whatsoever, one would expect a straight line at the 0 value across all dates; we do see some modest differences however, indicating that LEAPS operation at these 2 sites did affect the strength of stratification at the mid-lake monitoring station. The effect was a bit stronger when LEAPS was located at the Santa Rosa site, due no doubt in part to its closer proximity to the middle of the lake and site E2 (Fig. 1). Thus, LEAPS operation at the Santa Rosa site at a lake level of 1247' and with flows across the full face of the intake, weakened the thermal stratification by about 1.2 °C in late May and the beginning of June, with less of an effect other times of

the year (Fig. 23). Operation at the Ortega Oaks site had less of an effect, generally weakening stratification by <0.5 °C. Over the entire simulation period, operation of LEAPS at the Santa Rosa site altered thermal stratification on average only -0.05 °C, while the effect was even less for the Ortega Oaks site (-0.01 °C). The average values include intervals where LEAPS operation increased slightly the temperature at the mid-lake site (Fig. 23).

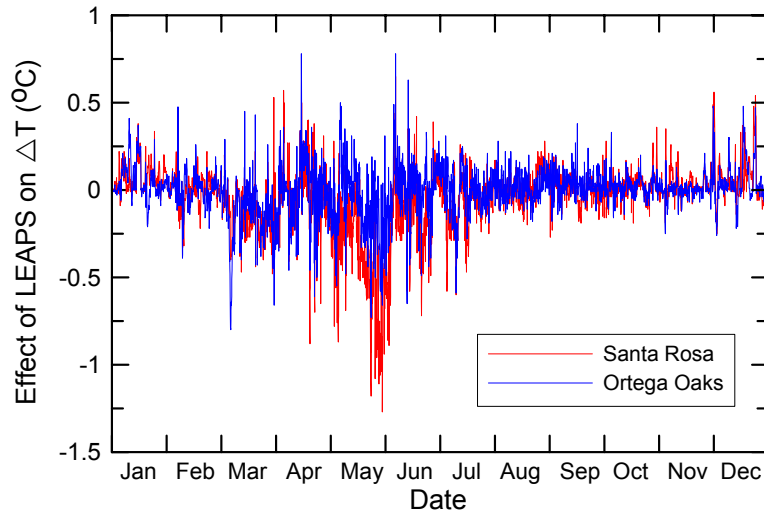


Fig. 23. Effect of LEAPS operation on predicted ΔT values normalized to those predicted for the lake without operation: flow across full wetted cross-sectional area, 1247 ft lake surface elevation.

Using the ΔT value at site E2 at 6:00 a.m. as our measure of the strength of stratification, we see that the lake was at least weakly stratified (defined here as $\Delta T > 1^\circ\text{C}$) for 121 days without LEAPS operation, while operation at the Santa Rosa and Ortega Oaks sites slightly decreased the number of days of weak stratification, to 110 and 116, respectively (Table 2). Operation of LEAPS at the Santa Rosa site also lowered slightly the number of days of strong stratification (taken here as $\Delta T > 3^\circ\text{C}$) from 51 days to 48 days and lowered the average duration of strong stratification from 8.5 days without LEAPS operation to 8.0 days (Table 2). Siting of LEAPS at Ortega Oaks did not affect the number of days of strong stratification nor its average duration relative to the reference case, however. Thus LEAPS operation at the Santa Rosa site had a small weakening effect on the predicted intensity and duration of stratification, while operation at the Ortega Oaks site had less of an effect. Neither meaningfully altered the predicted thermal properties of the lake at a surface elevation of approximately 1247', however.

Table 2. Intensity and duration of stratification at a lake elevation of 1247' with and without LEAPS operation.			
	No LEAPS	Santa Rosa	Ortega Oaks
$\Delta T < 1\text{ }^{\circ}\text{C}$ (mixed)	244 (66.8%)	265 (72.6%)	249 (68.2%)
$\Delta T > 1\text{ }^{\circ}\text{C}$ (stratified)	121 (33.2%)	110 (27.4%)	116 (31.8%)
$\Delta T > 3\text{ }^{\circ}\text{C}$ (strongly stratified)	51 (14.0%)	48 (13.2%)	51 (14.0%)
Average Duration ($\Delta T > 3\text{ }^{\circ}\text{C}$)	8.5	8.0	8.7

4.4.2 Stratification and Mixing at 1240 ft

Variation in lake level was shown to alter velocities near the intake and also influence bottom shear production; the intensity of stratification and frequency of mixing may also be affected.

The ΔT values calculated from predicted temperature profiles at site E2 at this lower lake level of 1240' were generally quite similar to those calculated at 1247'. The lake exhibited 2 weeks of relatively strong and continuous stratification in the latter part of March, with mixing in early April, followed by shorter intervals of stratification later in April and in early May (Fig. 24). The maximum ΔT value at 1240' was slightly lower than found at 1247', with LEAPS operation at the two sites weakening somewhat the strength of stratification at the end of March and in mid-May (Fig. 24), although the effect is subtle.

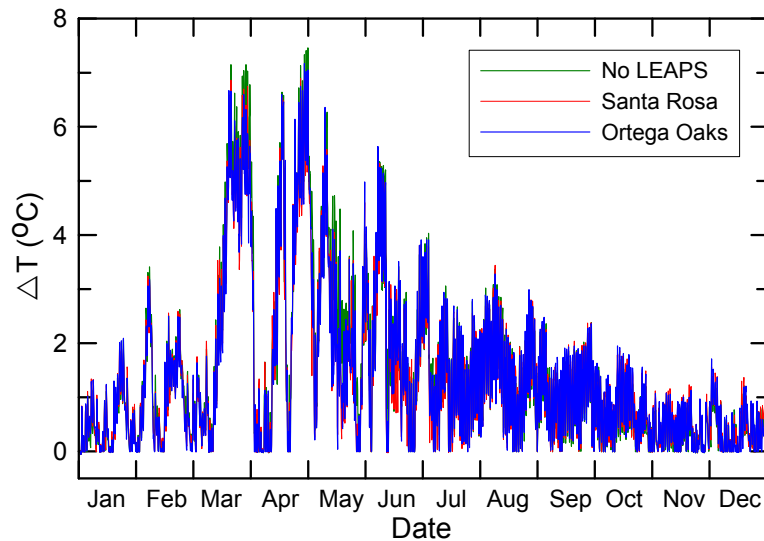


Fig. 24. Temperature differential (ΔT) between surface and bottom waters without LEAPS operation and operation at the Santa Rosa and Ortega Oaks sites, 1240 ft surface elevation.

To better highlight differences in the ΔT values calculated from LEAPS simulations at 1240' with those found at these lake levels without LEAPS operation, the difference between these values were again determined. As found at the higher lake level, operation of LEAPS (at either site) at 1240' had a modest effect on stratification (Fig. 25). LEAPS operation did lower the ΔT values predicted in May by about 1.5°C, an effect larger than predicted at 1247' (Fig. 23).

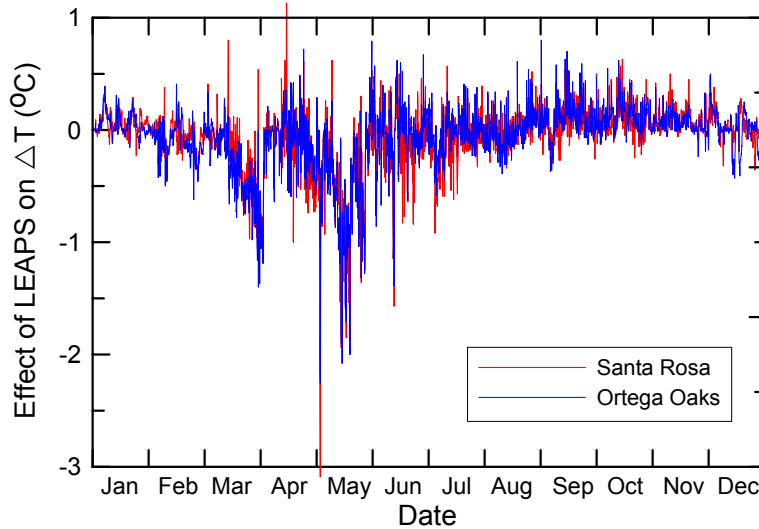


Fig. 25. Effect of LEAPS operation on predicted ΔT values normalized to those predicted for the lake without operation: flow across full wetted cross-sectional area, 1240 ft lake surface elevation.

Without LEAPS operation and under the meteorological conditions used in the simulation, the lake was predicted to be relatively well-mixed ($\Delta T < 1^\circ\text{C}$) 69% of the year at 1240' (Table 3), slightly more frequently than the 66.8% predicted for 1247' (Table 2). The average duration of strongly stratified conditions ($\Delta T > 3^\circ\text{C}$) at the lake was also predicted to decrease from 8.5 days at 1247' (without LEAPS) to 6.3 days at 1240'.

Table 2. Intensity and duration of stratification at 1240' with and without LEAPS operation.			
	1240'	Santa Rosa	Ortega Oaks
$\Delta T < 1^\circ\text{C}$ (mixed)	252 (69.0%)	273 (74.8%)	261 (71.5%)
$\Delta T > 1^\circ\text{C}$ (stratified)	113 (31.0%)	92 (25.2%)	104 (28.5%)
$\Delta T > 3^\circ\text{C}$ (strongly stratified)	38 (10.4%)	33 (9.0%)	35 (9.6%)
Average Duration ($\Delta T > 3^\circ\text{C}$)	6.3	6.6	7.0

We can thus conclude that lake level is overall a stronger determinant of the strength and duration of stratification than LEAPS operation, at least at when using the

proposed shoreline structure and at these 2 lake levels that have been proposed as the typical operational range for the project.

4.5 Selective Withdrawal

It was proposed by Horne (2005) that withdrawal and return flows at selected depths may be a way to more effectively weaken stratification and maximize DO levels above the sediments. To evaluate this, a series of additional simulations were conducted in which gate thickness and width were varied. That is, rather than flowing water through the full width and wetted height (that varies with lake level) of the intake, withdrawal and return flows were directed into specific depths using the withdrawal-return pair subroutine of EFDC (Hamrick, pers. comm.). While a large number of possible permutations could be evaluated, gate heights of 1 m were assumed with the lake level maintained at approximately 1247'. Pumping was assumed to withdraw water from near the middle of the water column (computational layer 4, corresponding to a depth of 4-5 m). Withdrawal from near the middle of the water column should help weaken local stratification by pulling water from the thermocline. Generation flows were directed alternately to the lowest vertical layer next to the rip-rap and bottom sediments or to the surface layer.

4.5.1 Velocities Near Intake

The local velocity field near the intake at the Santa Rosa site reflected this selective withdrawal and return (Fig. 26). Not unexpectedly, high velocities were predicted near the center of the water column adjacent to the intake during pumping (Fig. 26a). Velocities exceeding 12 cm/s were predicted at 4.6 m depth, with values declining both above and below this depth. Velocities near the bottom sediments declined to 3 cm/s, while flow at the surface slowed to 0.4 cm/s and actually reversed direction (i.e., unlike the other depths with flows directed toward the intake, the uppermost 1-m of water was predicted to move away from the intake during pumping) (Fig. 26a).

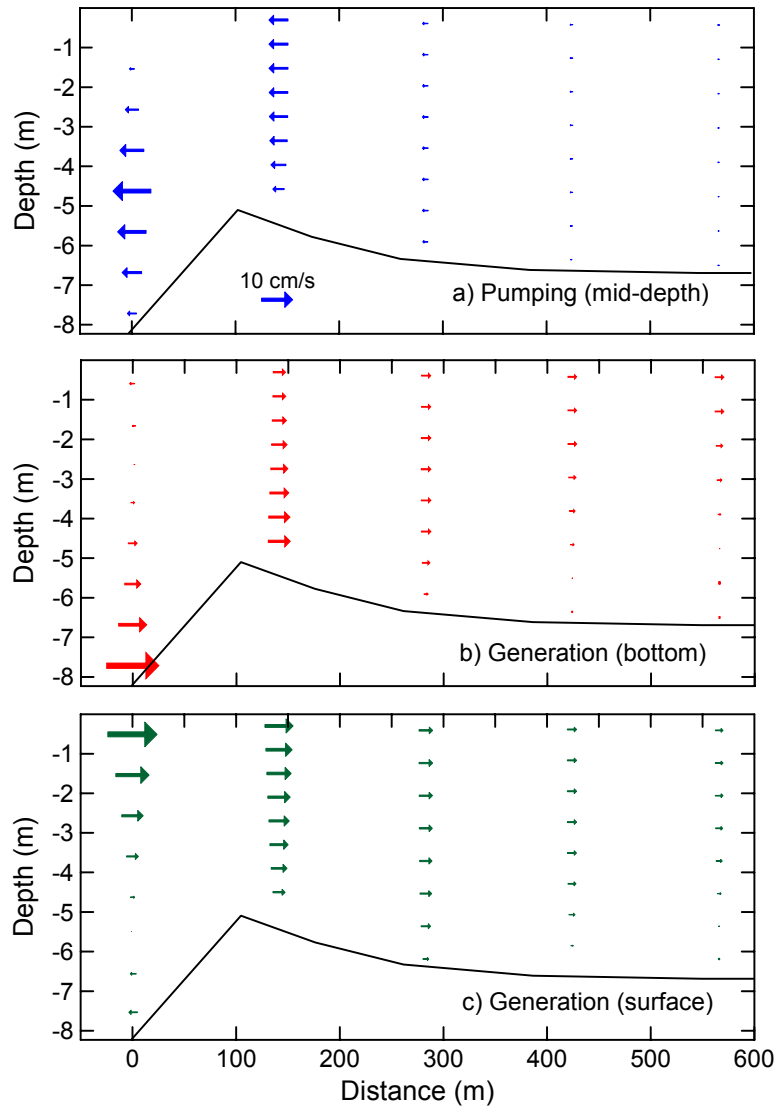


Fig. 26. Predicted velocity field perpendicular to the intake at the Santa Rosa site at 1247'. Active intake dimensions 150 m x 1 m, with a) withdrawal at 4-5 m depth, b) bottom generation (7-8 m depth), and c) surface generation (0-1 m depth). Note reference velocity scale in upper panel.

This strong vertical gradient in velocity was damped out quickly with distance, however, with much more uniform predicted velocity profiles, although lower velocities were still present near the sediments. For example, velocities varied from 3.65 cm/s near the sediments to 6.14 cm/s near the lake surface at 140 m distance from the intake (Fig. 26a). The depth-averaged velocity was nonetheless slightly higher at this distance than closer to the intake (5.55 vs. 5.49 cm/s, respectively). While velocities would be expected to decrease with distance as flows enter the lake, as previously discussed, the bottom topography forces water flow into a shallower region that, through conservation

of momentum, requires velocities to accelerate. Lateral flow (not shown in this transect) as well as frictional losses to the rip-rap and bottom sediments also dissipates available momentum. Depth-averaged velocities were observed to decrease at greater distances, however, to 2.73 cm/s at 280 m distance, 1.63 cm/s at 420 m, and 1.1 cm/s at 560 m (Fig. 26a).

Return flows directed to the bottom layer during generation resulted in high velocities near the sediments at the intake (16.8 cm/s) that decreased sharply away from the lake bottom (Fig. 26b). What is particularly interesting is the reversal of flow found in the uppermost 3 m of the lake adjacent to the intake (Fig. 26b). This indicates that a strong eddy with local short-circuiting of flow would be present under this operational scenario. The vertical gradient in velocity weakens with increasing distance from the intake, although the depth-averaged velocity increases from 4.0 cm/s near the intake to 5.4 cm/s 140 m downstream, before declining to 1.1 cm/s 560 m away (Fig. 26b).

Directing flows to the surface layer during generation resulted in velocities near the intake that decreased dramatically with depth, from 15.9 cm/s at the surface to 2.8 cm/s above the sediments (Fig. 26c). As found with bottom release, a flow reversal was found; here water in the bottom 3 m was flowing toward the intake so that an eddy was also predicted for surface generation flows. A stronger vertical gradient was in place away from the intake than the bottom release, however. For example, at 140 m downstream, surface currents were predicted to be 9.0 cm/s, with velocities declining to 3.9 cm/s above the sediment in this shallower region. Depth-averaged velocities declined to 3.7, 2.5 and 1.6 cm/s at 280-560 m away from the intake (Fig. 26c). Bottom velocities declined to <0.5 cm/s.

The effect of narrower intake structures that are more typical of pump-storage hydroelectric plants was also evaluated. In this simulation, a 1 m vertical gate was maintained, while the width of the intake was narrowed from 150 m to 40 m. Pumping water at equivalent flow rates through this narrower intake necessarily increased the velocities near the structure. Velocities of 20 cm/s were predicted for the 4.6 m depth; velocities declined to <0.1 cm/s within 3 m above or below this depth interval (Fig. 27a). Even with these high local velocities, however, predicted velocities declined to 0.5 cm/s 560 m away. Directing flows through the bottom 1 m of the intake yielded quite high velocities there (30.7 cm/s), with countercurrent flow setting up in the upper 4 m of the water column and reaching 7.7 cm/s at 0.5 m depth (Fig. 27b). Predicted velocities remained higher near the sediments than in prior simulations (Fig. 26), but still declined

with increasing distance from the intake (e.g., 0.8 cm/s above the sediments at a distance 420 m away) (Fig. 27b).

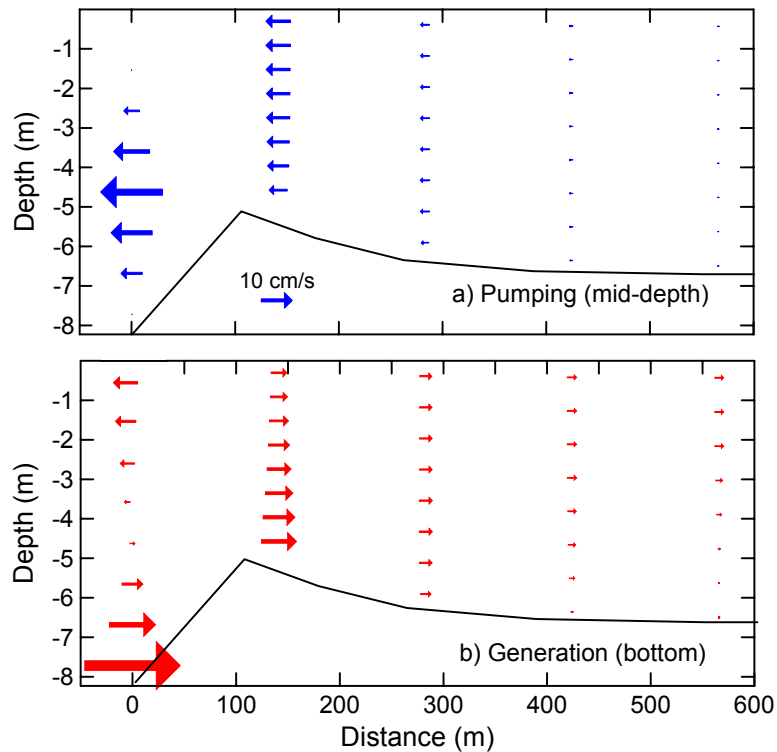


Fig. 27. Predicted velocity field perpendicular to the intake at the Santa Rosa site at 1247'. Active intake dimensions 40 m x 1 m, with a) withdrawal at 4-5 m depth, and b) bottom generation (7-8 m depth). Note reference velocity scale in upper panel.

A final set of simulations were conducted for the Santa Rosa site at a lake surface elevation of 1247 ft to evaluate the velocities profiles produced using a narrow (10 m) gate with a 1 m vertical opening. This small (10 m²) cross-sectional area would be similar to a single 3.6 m (or ~12 ft) diameter pipe. While locally very high velocities and strong counter-current flows are predicted near the intake (velocities up to 34 cm/s during pumping and 59 cm/s during bottom release generation), velocities nevertheless decreased markedly with distance from the intake (Fig. 28). The depth-averaged velocities at 560 m during pumping (3.4 cm/s) and generation (2.3 cm/s) were considerably higher than found under the other operational scenarios, however, reflecting the much smaller cross-sectional area available for flow.

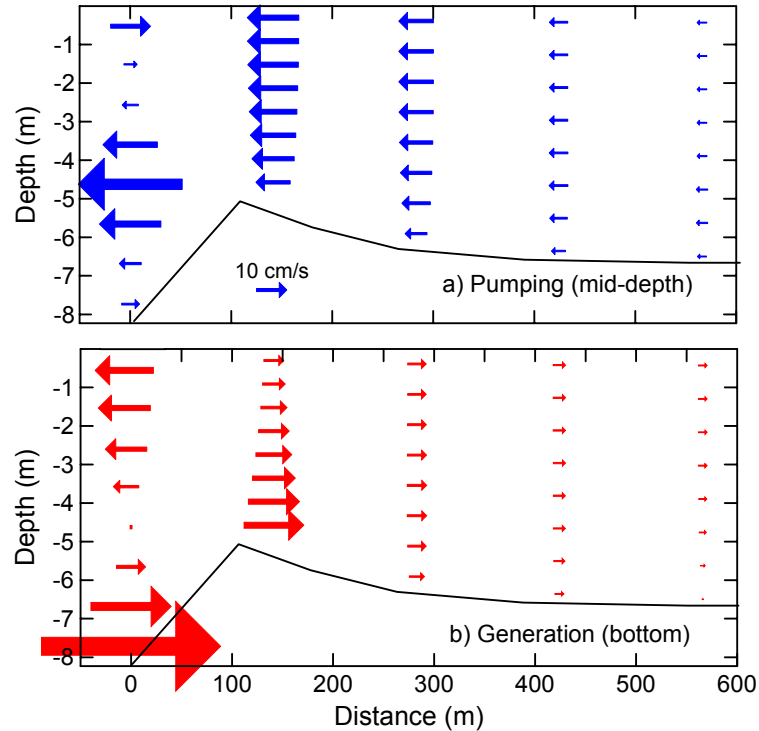


Fig. 28. Predicted velocity field perpendicular to the intake at the Santa Rosa site at 1247'. Active intake dimensions 10 m x 1 m, with a) withdrawal at 4-5 m depth, and b) bottom generation (7-8 m depth). Note reference velocity scale in upper panel.

Selective withdrawal and return flows were evaluated for the Ortega Oaks site as well. As previously noted, withdrawal during pumping was assigned to the 4th vertical layer from the bottom for these simulations. The effect of this was a predicted velocity profile similar to that found for the Santa Rosa site (Fig. 26a), with maximal velocities of 12.2 cm/s directed toward the intake at this depth, with velocities adjacent to the face of the intake decreasing both above and below this middle water column depth (Fig. 29a). In this configuration, velocities decreased to approximately 3 cm/s near the sediment, while velocities slowed and reversed direction near the surface (horizontal velocities of 0.4 cm/s away from the intake) (Fig. 29a).

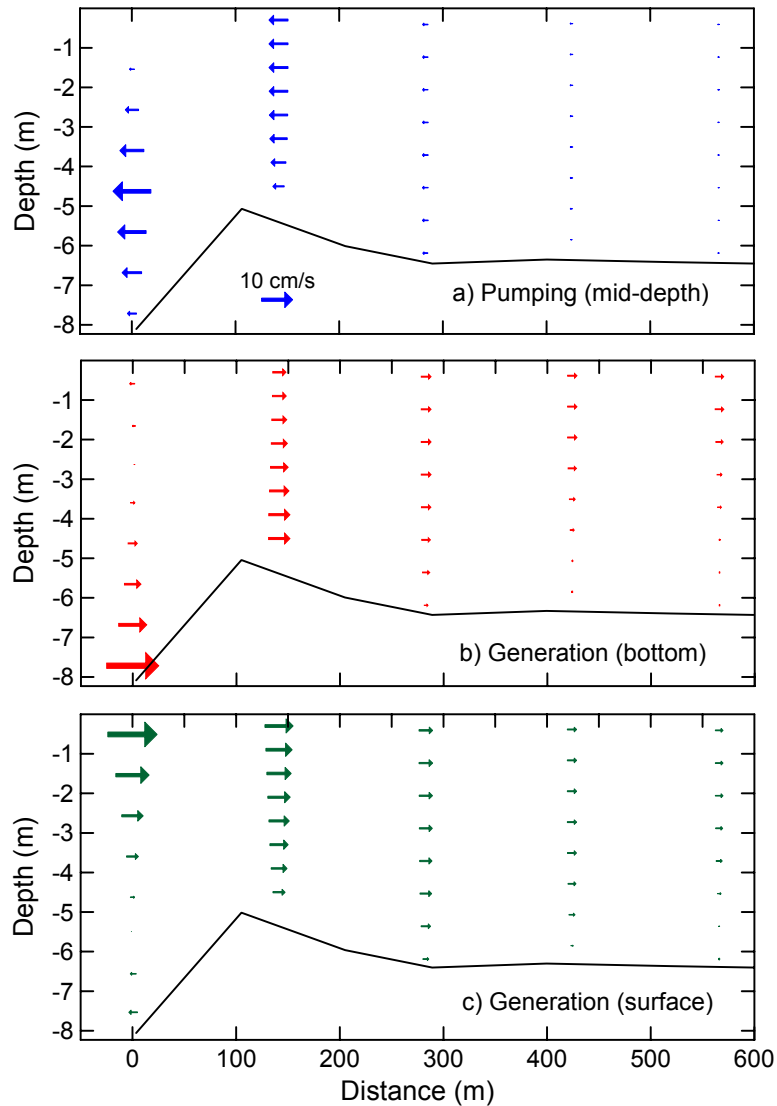


Fig. 29. Predicted velocity field perpendicular to the intake at the Ortega Oaks site at 1247. Active intake dimensions 150 m x 1 m, with a) withdrawal at 4-5 m depth, b) bottom generation (7-8 m depth), and c) surface generation (0-1 m depth). Note reference velocity scale in upper panel.

Thus there is some local short-circuiting of flow predicted during generation at this site, similar to that found at the Santa Rosa site. Out about 140 m from the intake, a more uniform velocity profile was predicted, with velocities ranging from 3.6 cm/s above the sediments to 6.1 cm/s near the lake surface. Depth-averaged velocities decreased with increasing distance from the intake, to about 1.8 cm/s at 280 m out perpendicular to the intake, to 0.76 and 0.47 cm/s at 420 and 560 m, respectively (Fig. 29a). Predicted velocities were generally slightly lower near the sediments when compared with other depths due to some frictional losses there. These velocities were taken from a simulation interval when natural wind-forcing was minimal to better illustrate the effects of LEAPS

operation on local circulation. Since velocities near this site are typically about 0.5 cm/s during the early morning, it would likely be difficult under most circumstances to identify flow effects due to pumping that extend out more than about 500 m from the intake.

The effects of generation on local velocity field was assessed for both bottom discharge (Fig. 29b) and surface discharge (Fig. 29c). Irrespective of depth of discharge, generation resulted in velocities opposite in direction to those predicted during pumping, i.e., directed *away from* the intake structure (e.g., Fig. 29b). Bottom discharge yielded predicted velocities near the sediments as high as 16.8 cm/s, although velocities decreased rapidly with distance above the sediments (Fig. 29b). The model in fact predicted a quiescent zone at a depth of about 2.5 m, above which flows reversed to 1.6 cm/s directed toward the intake. Thus, as found during generation, some local counter-current flows are expected to form during LEAPS operation. Velocities out 140 m from the intake were more uniform with depth, with the depth-averaged velocity at this distance from the intake (5.53 cm/s) actually slightly higher than that at the intake (4.1 cm/s), again due to the decreasing depth out about 100 m from the intake wherein conservation of momentum requires that the average velocity increase. Beyond this distance, velocities slowed to depth-averaged values of 2.7 at 280 m and 1.8 and 1.3 cm/s at 420 and 560 m, respectively (Fig. 29b). Bottom velocities were 30 – 90% lower than surface values, however, due in part to the physical obstruction of flow created by the sill formed from excavation of bottom sediment near the intake (Fig. 29b).

Surface discharge yielded velocity profiles that were essentially the mirror image of those found with bottom discharge. That is, high velocities directed away from the intake were present near the lake surface (15.9 cm/s) that decreased with depth until reversing direction in the bottom 2-3 m. (Fig. 29c) Velocities were more uniform 140 m from the intake, although they did vary from 3.9 cm/s near the sediments to 9.0 cm/s near the lake surface. Velocities slowed further at increasing distance as flows spread out away from the intake (Fig. 29c).

To assess the impact of smaller intake structures at the Ortega Oaks site, simulations were also conducted in which the intake gate was 40 m wide (Fig. 30) and 10 m wide (Fig. 31). As predicted for the Santa Rosa site, velocities near the intake were much higher when compared with those present when the full wetted cross-sectional area of the intake provided flow. For example, the 40 m wide intake gate yielded withdrawal velocities as high as 19.1 cm/s during pumping and discharge velocities as high 30.8 cm/s directed away from the intake during generation (Fig. 30). Strong

counter-current flows were set up near the intake during bottom discharge (e.g., predicted surface velocities toward the intake of 7.8 cm/s). Depth-averaged velocities were 20-60% higher 140 m from the intake than adjacent to the intake. Low velocities with some weak counter-current flows were predicted out past 400 m during bottom discharge (Fig. 30b).

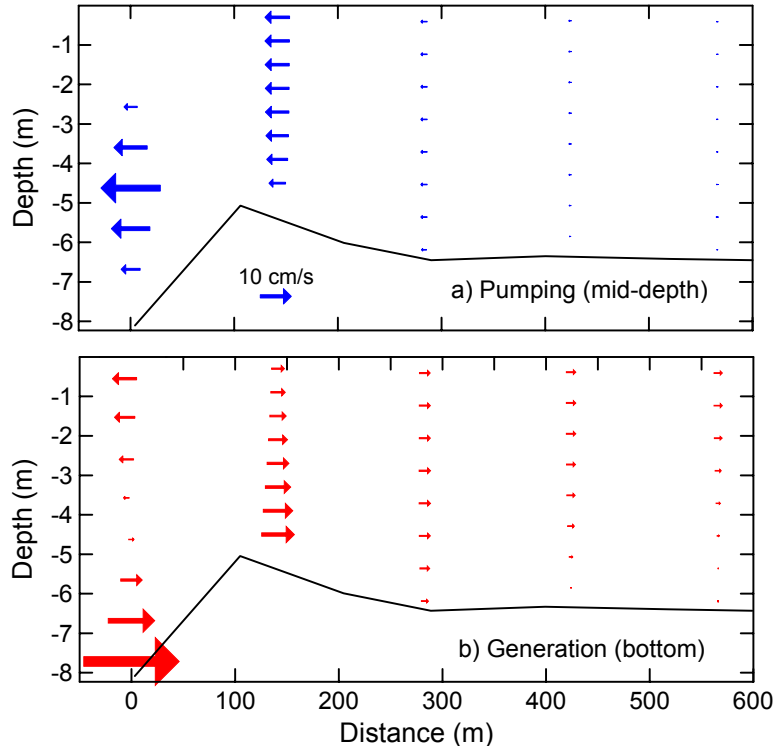


Fig. 30. Predicted velocity field perpendicular to the intake at the Ortega Oaks site at 1247'. Active intake dimensions 40 m x 1 m, with a) withdrawal at 4-5 m depth, and b) bottom generation (7-8 m depth). Note reference velocity scale in upper panel.

These effects were even more pronounced when a 10 m wide intake structure was used (Fig. 31). Pumping yielded predicted velocities >30 cm/s between 4-5 m depth, with flows reversing direction both near the sediments and near the surface of the lake (Fig. 31a). An even more dramatic counter-current flow was set up with bottom discharge. Under this scenario, bottom velocities were predicted to reach as high as 59 cm/s, with a thin quiescent shear layer at about 5 m depth and surface velocities as high as 20 cm/s and flowing in the opposite direction to that closer to the sediments (Fig. 31b). Interestingly, even at these high local velocities, the average velocities at 400-600 m from the intake (0.7-2.1 cm/s) were similar to those found in the wider intakes (1.3-1.8 cm/s).

The similarities between the velocity profiles found at the Santa Rosa and Ortega Oaks sites indicate that the structural and operational features of LEAPS dominates the flow regimes, and subtle bathymetric differences between the 2 sites have only small effects on predicted velocity fields at these lake elevations.

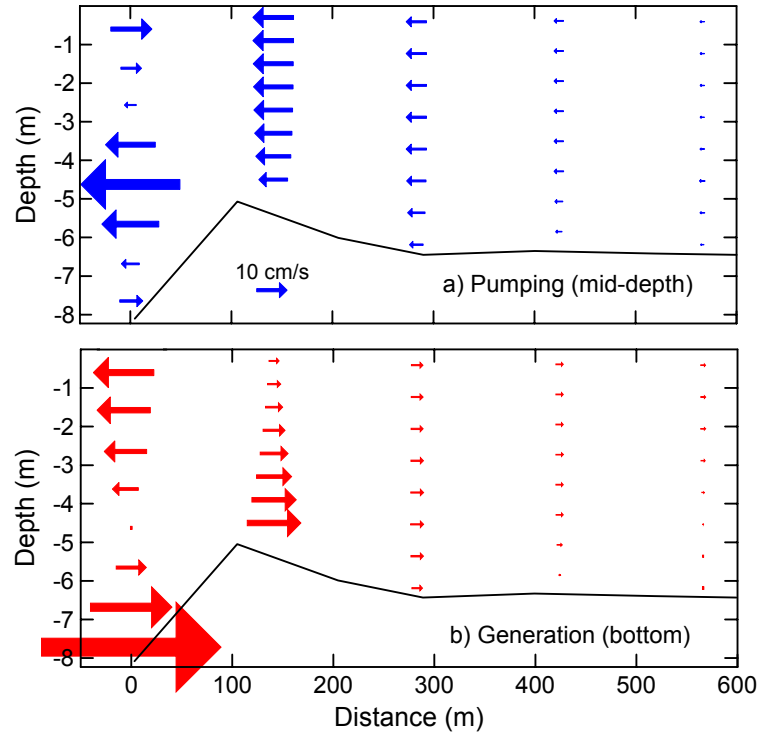


Fig. 31. Predicted velocity field perpendicular to the intake at the Ortega Oaks site at 1247'. Active intake dimensions 10 m x 1 m, with a) withdrawal at 4-5 m depth, and b) bottom generation (7-8 m depth). Note reference velocity scale in upper panel.

4.5.2 Bottom Shear and Sediment Resuspension

While LEAPS operation increased bottom shear near the intake, at nominal surface elevations of 1240 – 1247', predicted bottom shear remained below predicted critical values when flow was provided across the full wetted cross-sectional area of the intake (Figs. 18 and 19). Directing flow lower in the water column may help maintain aerobic conditions there, but the high predicted velocities are expected to generate substantial bottom shear. Bottom shear, in fact, exceeded critical values under these conditions (Fig. 32), where the colored regions represent the areas where $\tau > \tau_c$ (i.e., the regions of predicted sediment resuspension). Bottom shear for a 150 m x 1 m gate reached a maximum value of 0.38 N m⁻², while maximum shear values increased with decreasing gate width (1.3 and 5.5 N m⁻², respectively, for 40 m and 10 m gate widths) (Fig. 32).

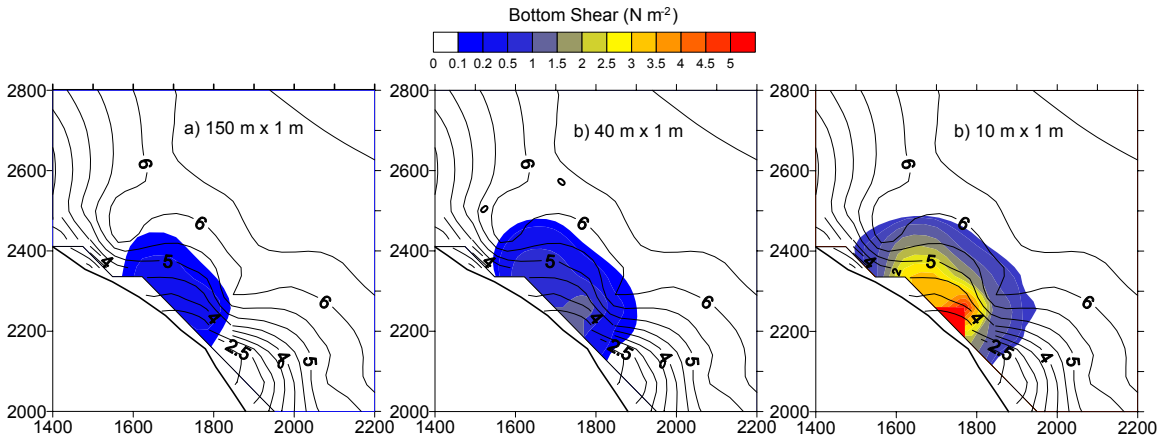


Fig. 32. Predicted bottom shear during generation at the Santa Rosa site (1247 ft lake surface elevation) for 3 different gate dimensions: a) 150 m x 1 m, b) 40 m x 1 m and c) 10 m x 1 m.

The average shear within the resuspension zone was inversely related to intake width, and increased from 0.28 N m^{-2} for a 150 m wide intake to 1.61 N m^{-2} for a 10 m intake gate (Table 2). The area of scour also increased from an estimated $38,000 \text{ m}^2$ to $80,000 \text{ m}^2$. More significantly, however, the mass of sediment scoured per unit area increased dramatically as a result of the exponential relationship in eq 1 (Table 4).

Intake Width x Height (m)	Area of Scour (m^2)	Average Shear (N m^{-2})	Scour (ϵ) (g m^{-2})	Total Mass Scoured (kg)	Local C_{ss} (mg/L)	Lakewide C_{ss} (mg/L)
150 x 1	38,000	0.24	4.5	170	0.99	0.002
40 x 1	61,000	0.54	138	8470	28.3	0.11
10 x 1	80,000	1.61	5612	4.39×10^5	1100	5.72

The total mass scoured increased with decreasing intake width due to both the very large increase in ϵ and the increase in area of scour, from 170 kg for the 150 m wide intake to 4.49×10^5 kg for the narrowest gate. The estimated suspended solids concentrations *within the resuspension zone* ranged from $<0.1 \text{ mg/L}$ to $1,100 \text{ mg/L}$ (Table 4). The concentration of suspended solids would decrease as a result of mixing with the rest of the lake, however. Assuming 3400 surface acres, a mean depth of 5.7 m and instantaneous mixing throughout the lake, the suspended solids concentrations would be below detection for all except the 10 m x 1 m gate configuration, where an instantaneous suspended solids concentration due to generation during LEAPS

operation would reach 5.72 mg/L (Table 4). It is recognized that the TSS concentration would be lower and rapidly decrease over time due to particle settling.

Predicted bottom shear at the Ortega Oaks site exhibited similar behavior and increased in both magnitude and spatial extent with decreasing gate width (Fig. 33). The area of resuspension ($\tau > 0.1 \text{ N m}^{-2}$) also increased.

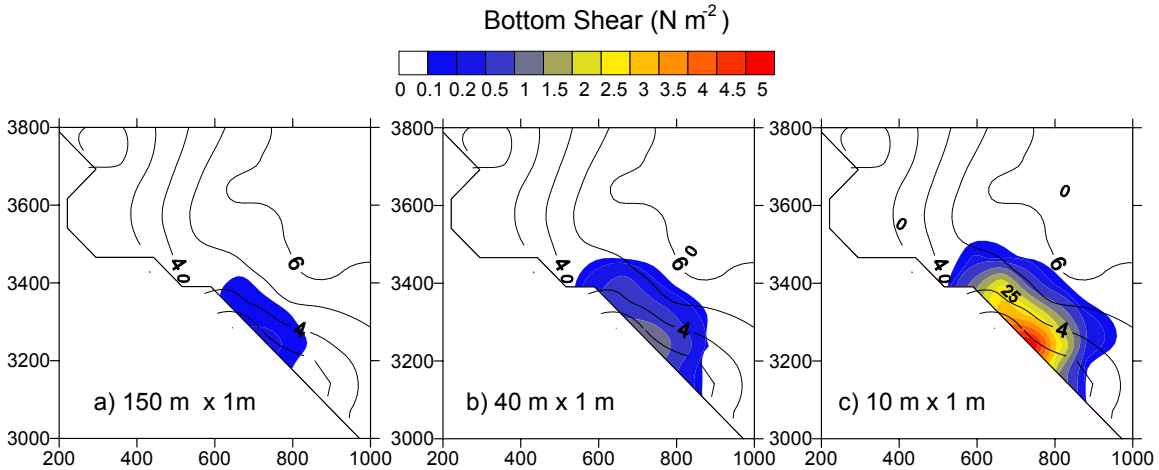


Fig. 33. Predicted bottom shear during generation at the Ortega Oaks site (1247 ft lake surface elevation) for 3 different gate dimensions: a) 150 m x 1 m, b) 40 m x 1 m and c) 10 m x 1 m.

The average shear within the resuspension zone was inversely related to intake width, and increased from 0.48 N m^{-2} at a 150 m x 1 m intake to a value of 2.78 N m^{-2} for a 10 m x 1 m intake (Table 5). The predicted area of scour also increased from $<5,000 \text{ m}^2$ to $83,000 \text{ m}^2$. More significantly, however, the mass of sediment scoured per unit area increased dramatically as previously noted, due to the exponential relationship in eq 1 (Table 5). The total mass scoured increased from 2030 kg for the 150 m wide intake to $2.60 \times 10^6 \text{ kg}$ for the narrowest intake. The estimated suspended solids concentrations *within the resuspension zone* ranged from $<0.1 \text{ mg/L}$ to $5,229 \text{ mg/L}$, while the theoretical lake-wide concentration ranged from <0.03 to 33.1 mg/L (Table 5).

Table 5. Predicted sediment resuspension at the Ortega Oaks site (1247 ft lake surface elevation)						
Intake Width x Height (m)	Area of Scour (m^2)	Average Shear (N m^{-2})	Scour (ϵ) (g m^{-2})	Total Mass Scoured (kg)	Local C_{ss} (mg/L)	Lakewide C_{ss} (mg/L)
150 x 1	22,700	0.48	89.4	2030	14.9	0.03
40 x 1	53,200	0.90	834	44,399	139	0.57
10 x 1	83,000	2.78	31,376	2.60×10^6	5229	33.1

These suspended solids concentrations are higher than predicted for the Santa Rosa site (Table 4). The somewhat shallower depths near the site resulted in only slightly higher velocities and bottom shear, but much higher mass of sediment potentially scoured from the bottom sediments (again following the cubic relationship between scour and difference between predicted and critical shear (eq 1)).

For comparison, the background TSS concentration in Lake Elsinore averaged 25.5 mg/L in 2003-2005, with >50% attributed to inorganic solids (Veiga-Nascimento and Anderson, 2005). Thus LEAPS operation is not predicted to substantially increase lake-wide suspended solids concentrations, even immediately after start-up. Chronic resuspension effects are not expected since the sediments will quickly come into equilibrium with the local velocity fields induced by LEAPS operation.

4.5.3 Stratification and Mixing

The effect of different intake configurations on the intensity of stratification at 1247' was also investigated. For example, bottom release of water through a 150 m intake with a 1 m slot width affected the relative strength of stratification in a manner quite similar to flows through the full face of the intake, although this configuration had less of an effect for the Santa Rosa site and a somewhat greater effect for the Ortega Oaks site (Fig. 34).

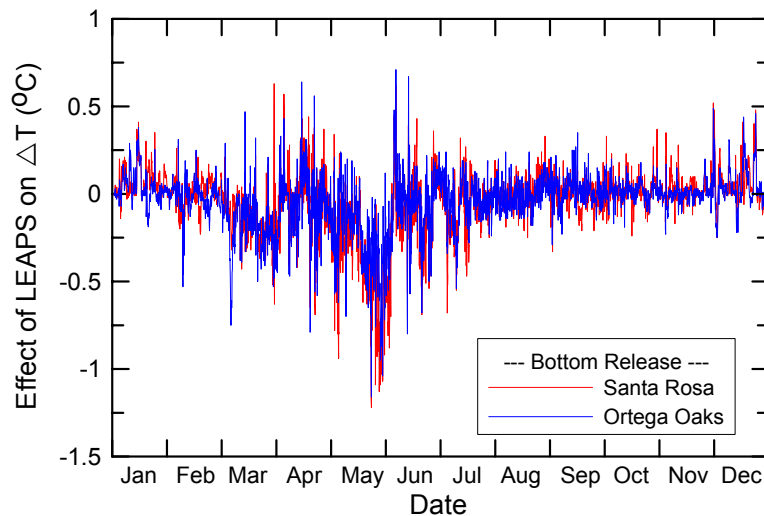


Fig. 34. Effect of LEAPS operation on predicted ΔT values normalized to those predicted for the lake without operation: 150 m x 1 m intake gate, bottom release, 1247 ft lake surface elevation.

The effect of intake width (previously shown to strongly influence bottom shear stress and sediment resuspension) had much less of an effect on far-field water column thermal properties (Fig. 35). That is, even gate widths as narrow as 10 m altered thermal stability in a manner similar to other configurations, although the effect was slightly greater than, e.g., 40 m (Fig. 30). For example, a 10 m x 1 m gate at the Ortega Oaks site altered average ΔT in late May by -0.71 °C, a value slightly larger than that for 40 or 150 m wide gates, that reduced ΔT values by -0.49 and -0.42 °C, respectively.

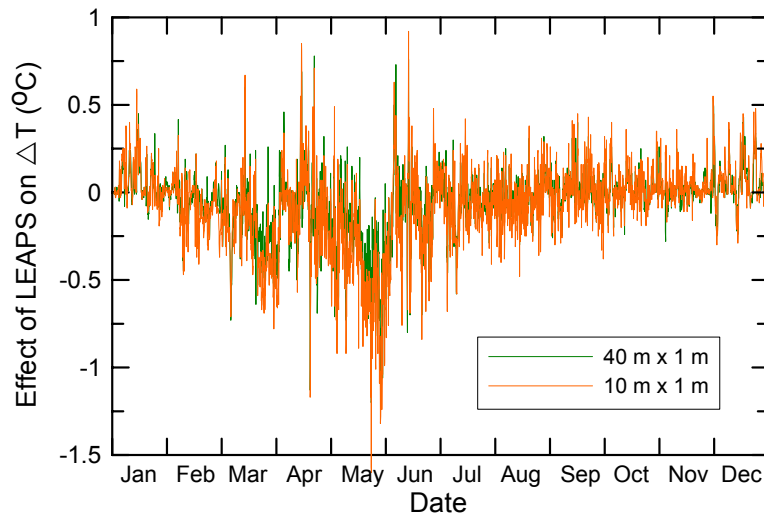


Fig. 35. Effect of LEAPS operation on predicted ΔT values normalized to those predicted for the lake without operation: 40 m x 1 m and 10 m x 1 m intake gate, bottom release, 1247 ft lake surface elevation.

The depth of discharge (surface, middle or bottom release) also yielded very similar (and minimal) effects on the strength of thermal stratification (not shown). For example, surface and bottom release at the Ortega Oaks site assuming a 150 m x 1 m intake both weakened average ΔT in late May by -0.42 °C, while mid-water column release weakened it by -0.46 °C.

5.0 Discussion

The hydrodynamic simulations provided valuable insights into the expected behavior and impacts of LEAPS operation on water column properties. While a number of different combinations of intake locations, configurations, and lake levels were evaluated, overall the effects of LEAPS operation on predicted water column properties were generally quite modest.

For example, irrespective of the specific location of the intake (Santa Rosa or Ortega Oaks sites), the operation of LEAPS increased local velocities only relatively short distances from the intake. The proposed shore-based intake design that is approximately 150 m wide and with a lower intake channel elevation of 1220 ft above MSL offers a very large cross-sectional area for flow, on the order of 1200 m² at a lake surface elevation of 1247'. This large cross-section keeps velocities low near the face of the intake. For example, the velocity adjacent to the intake at the Santa Rosa site during pumping at this lake surface elevation averaged 5.2 cm/s while a lower average velocity was predicted during generation (3.9 cm/s) due to the lower volumetric flow rate (Fig. 14). Velocities during generation increased somewhat out about 100 - 150 m perpendicular to the face of the intake due to the sill formed from excavation at the site. The decreasing depth away from the intake and toward the sill necessarily accelerated water velocities through this region. Velocities then slowed at greater distances, to average velocities of about 1 cm/s nearly 600 m from the intake. The predicted velocity profiles perpendicular to the intake located at the Ortega Oaks site were quite similar to those at the Santa Rosa site, with only slightly higher average velocities that reflect the somewhat shallower conditions near that site. For comparison, water velocities exceeding 1 cm/s are common throughout most of the lake, with velocities often exceeding 5 cm/s, especially in the southern end of the lake (e.g., Fig. 6).

These velocities did result in locally higher levels of bottom shear than typically found near the intake sites, at least under relatively quiescent conditions, although the levels remained below the assumed critical shear value of 0.1 N m⁻². The consequence of this is that sediment resuspension induced by LEAPS operation for this intake design and surface elevation (1247') is not expected to be a concern, especially with the emplacement of rip rap near the intake.

Moreover, the turbulent kinetic energy inputs into the lake as a result of pumping and generation were predicted to minimally alter stratification and mixing processes in the lake. Based upon predicted temperature profiles at a mid-lake location previously used in model calibration and validation (E2 in Fig. 1), the regular (5 day a week) operation of LEAPS over the year minimally altered the intensity and duration of stratification. Using the predicted temperature difference (ΔT) between the 2nd and 8th computational layer that corresponds to the 1.2 and 7.6 m depths at the site, operation of LEAPS at the Santa Rosa site weakened stratification by about 1.2°C in late May, but otherwise had generally little effect. Operation of LEAPS at the Ortega Oaks site

weakened thermal stratification $<0.5^{\circ}\text{C}$ over this same time period. In the absence of LEAPS operation and at a surface elevation of 1247', the lake was predicted to be at least weakly stratified ($\Delta T > 1^{\circ}\text{C}$ at 6:00 a.m.) for 121 days or one-third of the year, and more strongly stratified ($\Delta T > 3^{\circ}\text{C}$ at 6:00 a.m.) for 51 days (14.0% of the year). Operation of LEAPS at the Santa Rosa site slightly lowered the number of days each year with at least weak stratification, to 110 days, and with strong stratification to 48 days (13.2% of the year). The average duration of strong stratification also decreased slightly, from 8.5 days to 8.0 days. The effect of operation at the Ortega Oaks site was even smaller (the number of days with at least weak stratification decreased by 1.4%, with no effect on duration of strong stratification).

Based upon this, one can conclude that LEAPS operation using the proposed intake design near nominal maximum operating depth of 1247' will have minimal impacts on stratification, mixing and sediment resuspension in the lake. Modified densimetric Froude numbers previously calculated for the lake with LEAPS operation suggested that the lake would remain neither strongly stratified nor strongly mixed (Anderson, 2006b), and this 3-D hydrodynamic analysis supports this finding. The shore-mounted intake structure with a large cross-sectional area, combined with the recontoured lake bottom that yields a sill proximal to the intake, create low velocities and also appears to create sufficient turbulence to limit direct momentum flux into the deeper waters in the lake.

Comparable simulations were also conducted at a lake surface elevation of 1240', considered the nominal minimal operating elevation for LEAPS. The effect of a lower lake level reduces the depth of water at the face of the intake and thus also directly lowers the wetted cross-sectional area of the intake. On that basis, then, one would expect roughly 25% higher velocities near the intakes, although velocities increased by about 45%. This additional increase in velocity is attributed to greater channeling of flow perpendicular to the face of the intake due to the shallower neighboring sediment depths. Even greater acceleration over the shallow sill region was predicted, reflecting the greater relative change in depth there at lower lake surface elevations.

Shear stress increases as the square of velocity (Martin and McCutcheon, 1999), so the greater velocities predicted for 1240' produced substantially higher levels of bottom shear, e.g., a maximum bottom shear of 0.021 N m^{-2} was predicted adjacent to the intake during generation at the Ortega Oaks site at a surface elevation of 1247', while maximum bottom shear increased to 0.075 N m^{-2} at 1240'. The levels remained

below critical values, however, so even at the lower end of the expected operating surface elevation range, sediment resuspension is not expected to be a significant problem with this intake configuration.

The lower lake level was found to reduce the duration and intensity of stratification of the reference case (i.e., without LEAPS operation) compared with that predicted for 1247'. The number of days where ΔT exceeded 3 °C declined by almost 2 weeks, from 51 days per year at 1247' to 38 days at 1240'. The average duration of strong stratification also declined, from 8.5 days to 6.3 days. LEAPS operation had only a small incremental effect on duration of stratification, lowering the number of days where ΔT exceeded 3 °C by an additional 3-5 days. Strong stratification was predicted to persist an average of 6.6-7.0 days and still occur 33-35 days each year.

LEAPS was predicted to have more dramatic effects on velocities and bottom shear near the intake when withdrawal and return flows were focused into discrete depths there. For example, reducing the gate height at the Santa Rosa site from the full water depth at the intake (approximately 6-8 m at 1240-1247') to a 1 m slot width substantively altered the velocity profiles. Velocities exceeding 12 cm/s were predicted during pumping from mid-depth within the water column, while surface and bottom release during generation yielded velocities of 16 – 17 cm/s. The model further predicted counter-current flows setting up, e.g., flows toward the intake during generation when bottom release was employed.

Narrowing the intake from the 150 m to 40 m while maintaining a 1 m slot width yielded even greater velocities (20 – 30 cm/s during pumping and generation, respectively), with a more pronounced countercurrent flow regime in place. Narrowing the intake further, to 10 m width, produced velocities of 34 cm/s during mid-depth pumping and 59 cm/s during bottom release generation, with dramatic countercurrent flows (exceeding 19 cm/s and directed toward the intake during generation). These velocities would create entrainment concerns not only for larval fish and other planktonic organisms but also would likely entrain weak swimming juveniles and some adults as well.

Despite the high velocities near the intake, water currents slowed dramatically away from the intake, such that even with velocities approaching 60 cm/s at the intake, values declined to <3 cm/s at 560 m distance; this is a velocity lower than values often seen in lake under typical daily meteorological conditions.

The high velocities near the intake due to use of narrow gates and slot widths did generate a great deal of bottom shear stress however, such that an estimated 22,700 – 83,000 m² (6 - 21 acres) of lake bottom could be prone to resuspension. While the 150 m x 1 m intake gate was predicted to scour little sediment (170 and 2030 kg for the Santa Rosa and Ortega Oaks sites, respectively), the very narrow 10 m x 1 m intake gate with bottom release was predicted to scour in excess of 2,600,000 kg at the Ortega Oaks site. Despite the high local velocities, even these narrow intake gates and slot widths had a minimal influence on thermal stratification, lowering for example, ΔT at site E2 by 0.49 – 0.71 °C for 40 m and 10 m intake gate widths when operated at the Santa Rosa site.

The focusing of flow to discrete depths within the water column through the use of gate structures appears to offer little benefit. Selective withdrawal and return flow was not predicted to substantively weaken stratification or improve mixing in the lake. Moreover, a very narrow gate was predicted to create velocities of sufficient magnitude that entrainment of nearby free-swimming organisms would be possible during pumping, while bottom release through a very narrow gate could unnecessarily create sediment resuspension problems, at least upon initial start-up and after intervals of non-operation.

6.0 Conclusions

Model simulations indicate that LEAPS is not predicted to substantially alter the natural stratification and mixing processes in the lake, nor resuspend significant quantities of sediments unless a very narrow gate structure is used. These are rather surprising results in some ways, since a substantial amount of turbulent kinetic energy is introduced to the water column during operation (Anderson, 2006). Two factors are thought to account for these observations. First of all, previous heat budget calculations (Anderson 2006b) indicated that LEAPS operation is not expected to alter the temperature of the water returned during generation. Thus, strong overflow or underflow conditions due to differences in density of water delivered to the lake are not expected. That is, water will be removed and returned to equivalent depths during operation; as a result, buoyant forces would not be able to focus flow to narrow depth regions that could allow water to move comparatively large distances from the intake at higher velocities relative to flow mixed into a larger vertical region.

The 2nd factor that is thought to greatly affect observed behavior concerns the bottom topography near the intake. Since the intake is a shore-mounted structure, it is

located in shallow water that requires removal of an estimated 24,000 – 26,000 m³ of sediment. This excavation will create a substantial sill located approximately 100 m into the lake (Figs. 11 and 12). Water withdrawn or returned through the intake flows over the sill and thus water will be added to or removed from the upper water column (the upper ~5 m when the lake is at 1247' and the uppermost ~3 m when the lake level is near the lower operational range of 1240'). Moreover, the sill that necessarily encircles the intake tends to promote a high degree of turbulence and formation of eddies and counter-current flows that further restrict efficient transfer of momentum into the deeper portions of the lake. These factors thus limit the potential for enhanced mixing of the water column away from the immediate effect of the intake.

7.0 References

Anderson, M.A. 2006a. *Analysis of the Potential Water Quality Impacts of the LEAPS Project on Lake Elsinore*. Report submitted to the Santa Ana Regional Water Quality Control Board. 30 pp.

Anderson, M.A. 2006b. *Lake Heating, Cooling and Stratification During LEAPS Operation*. Report submitted to the Santa Ana Regional Water Quality Control Board. 25 pp.

FERC, 2006. Draft Environmental Impact Statement for Hydropower License: Lake Elsinore Advanced Pumped Storage Project. FERC Project No.11858. FERC/EIS-0191D. 494 pp.

Hamrick, J.M. 1992. *A three-dimensional environmental fluid dynamics computer code: Theoretical and computational aspects*. Spec. Re. No. 317, The College of William and Mary, Virginia Institute of Marine Science, VA.

Horne, A. 2005. Memo to David Kates. Re: FERC questions on effects of lake level changes due to the proposed hydropower generation on Lake Elsinore water quality. 8 pp.

Jin, K.-R. and Z.G. Ji. 2005. Application and validation of three-dimensional model in a shallow lake. *J. Waterway, Port, Coastal, Ocean Engin.* 131:213-225.

Martin, J.L and S.C. McCutcheon. 1999. *Hydrodynamics and Transport for Water Quality Modeling*. Lewis Publ., Boca Raton, FL. 794 pp.

THNC (The Nevada Hydro Company). 2004. Deficiency Letter Response. FERC Project No. 11858-002. Clarification (8).

USEPA. 2007. TMDL Modeling Toolbox. <http://www.epa.gov/athens/wwqtsc/Toolbox-overview.pdf>.

Veiga-Nascimento, R. and M.A. Anderson. 2004. *Lake Elsinore Recycled Water Monitoring Project. Final Report*. Submitted to Lake Elsinore-San Jacinto Watersheds Authority. 59 pp.

This page intentionally left blank.